

# Entanglement Entropy and Quantum Phase Transition in the $O(N)$ $\sigma$ -model

Jiunn-Wei Chen\*

*Department of Physics and Center for Theoretical Sciences,  
National Taiwan University, Taipei 106319, Taiwan  
Leung Center for Cosmology and Particle Astrophysics,  
National Taiwan University, Taipei 106319, Taiwan  
Physics Division, National Center for Theoretical Sciences,  
National Taiwan University, Taipei 106319, Taiwan and  
Center for Theoretical Physics, Massachusetts  
Institute of Technology, Cambridge, MA 02139, USA*

Shou-Huang Dai<sup>†</sup>

*Center for General Education, Southern Taiwan University  
of Science and Technology, Tainan 710301, Taiwan*

Jin-Yi Pang<sup>‡</sup>

*University of Shanghai for Science and Technology, Shanghai 200093, China and  
Department of Physics and Center for Theoretical Sciences,  
National Taiwan University, Taipei 106319, Taiwan*

## Abstract

We investigate how entanglement entropy behaves in a non-conformal scalar field system with a quantum phase transition, by the replica method. We study the  $\sigma$ -model in 3+1 dimensions which is  $O(N)$  symmetric as the mass squared parameter  $\mu^2$  is positive, and undergoes spontaneous symmetry breaking while  $\mu^2$  becomes negative. The area law leading divergence of the entanglement entropy is preserved in both of the symmetric and the broken phases. The spontaneous symmetry breaking changes the subleading divergence from log to log squared, due to the cubic interaction on the cone. At the leading order of the coupling constant expansion, the entanglement entropy reaches a cusped maximum at the quantum phase transition point  $\mu^2 = 0$ , and decreases while  $\mu^2$  is tuned away from 0 into either phase.

## I. INTRODUCTION

Entanglement[1] is an intriguing feature of Quantum Mechanics. Its has become increasingly important in quantum information[2], condensed matter[3–6], string theory[7], and the interpretation of black hole entropy[8]. For example, in the condensed matter systems, the ground states of the conventional superconductors[9, 10] and the fractional quantum Hall effect[11] are both entangled states. The level of the entanglement between a certain region and its surroundings is measured by the entanglement entropy. Such systems may undergo quantum phase transition at zero temperature by tuning their physical parameters. The quantum phase transition[12] is fundamentally different from the conventional thermal phase transition occurred at non-zero temperature as the former involves a qualitative change of the ground state of a quantum system. In this paper, we are particularly interested in the insight about the quantum phase transition from the point of view of the entanglement entropy.

Traditionally, different phases are classified by the order parameters keeping track of the symmetries broken in the phase transitions. Valuable insights on the change of the symmetry and the degrees of freedom in a phase transition can be obtained by the symmetry breaking order parameters and thermal dynamical variables, respectively, both of which can be studied

---

\* jwc@phys.ntu.edu.tw

† shdai@stust.edu.tw

‡ axial.pang@gmail.com

in thermal equilibrium. On the other hand, by means of the transport coefficients, one can also study how a phase transition affects the real time responses of the system perturbed slightly away from thermal equilibrium. One example is the shear viscosity ( $\eta$ ) over the entropy density ( $s$ ). At the phase transition temperature of a scalar field system, this  $\eta/s$  ratio tends to minimize locally; the minimum has a smooth structure for a crossover, forms a cusp for a second order phase transition, and has a jump for a first order phase transition [13]. This behavior is seen in many systems in nature and many theoretical models. However, counter examples can be engineered [14].

We aim to pursue analogous understanding on the behavior of the entanglement entropy under the quantum phase transitions in the present research. As the entanglement entropy scales with the area of the interface between two entangled regions, at finite temperatures it becomes subleading compared with the thermal entropy which scales with the volume of the system. The quantum phase transition studies involving the entanglement entropy had focused on the zero temperatures cases, in particular the lattice systems. For example, previous work on the 1+1 dimensional transverse Ising model shows the entanglement measure reaches a local maximum at the second order quantum phase transition [3, 6]. Studies on various spin chain models in 1+1 dimensions also reveal the universal scaling behaviors of the ground-state entanglement near the quantum critical point [4, 5]. For a broader review on the entanglement properties in many-body systems, see e.g. [15].

As for the systems of the scalar fields in the continuum, through the study of the conformal cases [16–21] and the non-conformal cases [17, 22], it is known that the entanglement entropy ( $S_{\text{ent}}$ ) between a subregion  $A$  and its complement  $\bar{A}$  of the spacetime has a leading behavior exhibiting the power law divergence and the area law[23],  $S_{\text{ent}} \sim \Lambda^{d-1} A_{\perp}$ , where  $A_{\perp}$  is the area of the  $d - 1$  dimensional boundary of  $A$ , with  $d$  denoting the number of spatial dimensions and  $\Lambda$  is the momentum cutoff. For the non-conformal scalar field theory to our particular interest in this paper, the subleading part of the entanglement entropy, according to [22] which deals with a single-component massive scalar field in 3+1 dimensions with both the cubic and the quartic self-couplings, contains the  $\lambda A_{\perp} \Lambda^2$  term arising from the quartic interaction  $-\frac{\lambda}{4!}\phi^4$ , and the  $g^2 A_{\perp} \ln(\Lambda^{-1})$  term from the cubic interaction  $-\frac{g}{3!}\phi^3$ , where  $\lambda$  and  $g$  are bare couplings. They are contributed by the two-loop quantum corrections, and can be absorbed into the mass renormalization of  $\phi$ . As a result, the subleading part of  $S_{\text{ent}}$ , e.g.  $\frac{1}{48\pi} A_{\perp} m_r^2 \ln m_r^2$ , where  $m_r$  stands for the renormalized mass of the scalar field, becomes

cutoff-independent, such that as  $m_r$  varies, the change in the entanglement entropy is cutoff independent and thus physical.

In this paper, we investigate how the entanglement entropy behaves in the quantum phase transition of a scalar field system in the continuum under the spontaneous symmetry breaking (SSB), by the path integral approach and the replica trick. The theoretical model we explore is the  $O(N)$   $\sigma$ -model, which is a weakly coupled  $N$ -component scalar field theory, in 3+1 dimensions<sup>1</sup>. Our scalar fields live in a bipartite infinite flat spacetime, where each of the semi-infinite half-spaces is denoted by  $A, \bar{A}$ . In the  $O(N)$  symmetric phase, Our model has the quartic interactions  $\frac{\lambda}{4} \left[ \sum_{i=1}^N (\phi^i)^2 \right]^2$  as the mass squared  $\mu^2$  of  $\phi^i$  is positive. By tuning  $\mu^2$  from positive to negative, the  $O(N)$  symmetry is spontaneously broken into  $O(N-1)$ , and the field composition of the system turns into a massive mode  $\sigma$  with a mass  $m_\sigma = \sqrt{-2\mu^2}$ , and  $N-1$  massless Goldstone bosons  $\pi^i$ 's. In the broken phase the cubic interactions  $\frac{1}{\sqrt{2}} g m_\sigma \left( \sum_{i=1}^{N-1} (\pi^i)^2 \sigma + \sigma^3 \right)$  emerge, where  $g = \sqrt{\lambda}$ . This phase is characterized by the emergence of a non-trivial order, i.e. a non-trivial scalar field VEV. As the SSB occurs, the system undergoes a quantum phase transition under which the vacuum states change. We are interested in the leading and subleading UV divergences of the entanglement entropy in this paper. We will apply the replica method and the field theory expansion technique on the cone, to analyze the effect of the quantum phase transition on the entanglement entropy in the  $O(N)$   $\sigma$ -model due to the SSB. This is a perturbatively calculable system due to weak coupling, and we present our result up to two-loop corrections. To achieve our goal, we apply some of the approximation technique from [22] to the calculation in our symmetric phase. However, in the broken phase, the calculation method we use is different from [22], and hence the result; this will be explained later in this Section.

We summarize our result of the entanglement entropy divergence structures for the  $\sigma$  model in the  $O(N)$  symmetric and the broken phase below, according to our renormalization scheme up to two-loop level:

$$S_{\text{ent.}}(\mu^2, \lambda) = \frac{A_\perp N}{48\pi} \left\{ (\ln 4) \Lambda^2 + a \tilde{\lambda} |\mu^2| \left( \ln \frac{|\mu^2|}{\Lambda^2} \right)^2 + (b + c \tilde{\lambda}) |\mu^2| \ln \frac{|\mu^2|}{\Lambda^2} + O \left( \tilde{\lambda}^2, \frac{|\mu^2|}{\Lambda^2} \right) \right\}, \quad (1)$$

where the coefficients  $a, b, c$  are given by

---

<sup>1</sup> This type of models had been extensively studied on their thermal phase transition properties, e.g. providing a controlled perturbation to probe  $\eta/s$ . See for example [13, 24, 25].

	$O(N)$ symmetric	Spontaneous Symmetry Broken Phase
a	0	$-\frac{3}{(4\pi N)^2}(N+2)$
b	1	$\frac{2}{N}$
c	0	$-\frac{2}{(4\pi N)^2}\{9\sqrt{5}\ln(\frac{3+\sqrt{5}}{2})+(6\ln 2-2)+(3\ln 2+2)N\}$

In these expressions,  $N$  is the number of species of the scalar fields, and  $\tilde{\lambda} = \lambda/N$ . Note that  $\mu$  and  $\lambda$  all stand for the renormalized parameters. The area law is clearly observed, with  $A_\perp$  denoting the area of the 2-dimensional boundary surface of  $A$ . There is also the momentum cutoff  $\Lambda$  dependence in the leading divergence.

The  $a$ ,  $b$  and  $c$  coefficients can be extracted from (where  $\bar{\Lambda}$  is some arbitrary cut-off)

$$\begin{aligned}
a &= \frac{\partial^2}{(\partial \ln |\mu^2|)^2} \frac{\partial}{\partial |\mu^2|} \frac{24\pi S_{\text{ent.}}}{A_\perp N \tilde{\lambda}} \\
b + c\tilde{\lambda} &= \frac{\partial}{\partial \ln |\mu^2|} \frac{\partial}{\partial |\mu^2|} \left[ \frac{48\pi S_{\text{ent.}}}{A_\perp N \tilde{\lambda}} - a|\mu^2| \left( \ln \frac{|\mu^2|}{\bar{\Lambda}^2} \right)^2 \right].
\end{aligned} \tag{2}$$

(1) is obtained by using the renormalized mass, coupling constant and fields at the tree level, and introduce the counter terms to cancel the quantum loop corrections, in contrast to [22]. The counter terms in the symmetry broken phase and those in the  $O(N)$  symmetric phase are of the same origin (c.f. Appendix).

(1) shows that the area law is the leading behavior of the entanglement entropy in both phases, which is expected. In the symmetric phase, the quartic interactions give rise to the subleading non-analytic structure  $|\mu^2| \ln \frac{|\mu^2|}{\bar{\Lambda}^2}$  at  $O(\tilde{\lambda}^0)$ , agreeing with the result of [22]. In the broken phase, however, a new log squared term  $|\mu^2| \left( \ln \frac{|\mu^2|}{\bar{\Lambda}^2} \right)^2$  emerges at  $O(\tilde{\lambda})$ , which is more divergent than log. This term is never seen in previous literature, including [22]. This term arises from the remnant of cancellation between the two-loop expansions of the cubic interactions (emerged due to the SSB) and the counter term. The Goldstone-Goldstone and the Goldstone-massive mode quartic interactions give rise to the single log divergence (at  $O(\tilde{\lambda})$ ) and become sub-subleading.

The origin of the log squared term is explained as follows. We find that the approximation used in [22] for integrating the sunset diagrams on the cone due to the cubic interactions are over-simplified. Careful treatment of those diagrams in our work yields the double logarithm behavior of the entanglement entropy in the broken phase. To explain this schematically, [22] calculates the Green's function  $G_n(x, x')$  on the cone by assuming that the leading divergence is dominated by  $x \rightarrow x'$ , such that the sunset diagram becomes approximated by

the two-loop diagram with one vertex. The divergence from one of the loops is then canceled by the counter terms, leaving the single log behavior. However, our analysis shows that the “ $x$  away from  $x'$ ” part of the sunset diagrams on the cone should be taken into account, and as a result the divergence cannot be canceled by the counter terms, yielding the double log structure in the broken phase. We refer the readers to Sec. VI for a more in-depth explanation, and to the Appendix for the detail of the calculation. We also argue that the log and the double log structures are independent of the renormalization schemes, as they are of order  $\tilde{\lambda}$  quantities, while the influence of different schemes takes effect at  $O(\tilde{\lambda}^2)$  or higher.

The other difference between our work and [22] is in the system setup. [22] employs a massive single-component scalar field with  $-\frac{g}{3!}\phi^3 - \frac{\lambda}{4!}\phi^4$  interactions. Our model deals with a  $N$ -component massive scalar field in the symmetric phase with only the quartic interactions, while in the broken phase due to SSB, the massless Goldstone bosons and a massive  $\sigma$  field emerge, and the cubic interactions between them naturally arise beside the quartic ones, in which the massive scalar mode and the massless Goldstone bosons couple together. In this sense, our work generalize the result of [22]. If we take  $N = 1$ , our model simplifies to [22]’s setup, as the massless Goldstone bosons disappear. But in the broken phase, (1) doesn’t reduce to [22]’s result because we don’t take  $x \rightarrow x'$  approximation for the Green’s function on the cone, as mentioned above.

Moreover, our work also present the novel result in the numerical behavior of the entanglement entropy of the  $O(N)$   $\sigma$ -model under the quantum phase transition due to the SSB. The scaling behavior of the entanglement entropy thus can be spelled out from (1). (See Sec. V for details.) We find the entanglement entropy reaches its maximum with a cusp at the transition point  $\mu^2 = 0$ . While  $|\mu^2|$  shifts away from 0 into either phase, the entanglement entropy decreases as the correlation length reduces away from the quantum critical point, as shown in Fig. 4. Although our result of the entanglement entropy change in Fig. 4 is numerical, it would be interesting if an analytic expression of the universal scaling behavior near the transition point can be unveiled.

In our  $O(N)$  sigma model, the phases are classified by the nontrivial order  $\langle\phi^N\rangle$ . Besides this SSB-driven quantum phase transitions, there are also phase transitions which do not involve any “local” order parameters. One example is the topologically ordered phases [26]. In these cases, the entanglement entropy remains an important quantity identifying the

topological order [27, 28]. The entanglement entropy contains a part called the topological entanglement entropy [29, 30], which varies in different topological phases. Such systems, however, are beyond the scope of this paper.

The structure of this paper is organized as follows. We first review in Sec. II the fundamentals of the entanglement entropy and the replica method in quantum field theory. Sec. III presents the entanglement entropy of  $O(N)$   $\sigma$ -model in the  $O(N)$  symmetric phase, up to two-loop perturbations. Sec. IV performs analogous calculation for the broken phase. Sec. V presents the numerical behavior of the entanglement entropy versus  $\mu^2$  in both phases. The entanglement entropy has a cusped maximum at the quantum phase transition point. Sec. VI. discusses and concludes our work, and presents potential future applications. The Appendix presents the calculation details in deriving the divergence structures of the entanglement entropy.

## II. ENTANGLEMENT ENTROPY AND REPLICA METHOD

The thermal entropy indicates the level of disorder of a system. In the quantum case, the thermal entropy is given by the von Neumann entropy

$$S = -\text{Tr}[\rho \ln \rho], \quad (3)$$

where  $\rho$  is the density matrix which is normalized to  $\text{Tr}\rho = 1$ . In the diagonalized basis, the von Neumann entropy reads  $S = -\sum_i p_i \ln p_i$ , where  $p_i$  is the probability for each microstates being occupied. By postulating the occupation of any microstate is equally probable, (3) is equivalent to the statistical definition of the entropy  $S \sim \ln \Omega$  up to the Boltzmann constant, reflecting the total number of accessible microstates in a quantum system of microcanonical ensemble.

Consider a bipartite system  $S$  in a pure state and composed of subsystems  $A$  and  $\bar{A}$ , where the degrees of freedom in  $A$ ,  $\bar{A}$  are entangled in some way. If one is forbidden to access  $\bar{A}$ , then for such an observer,  $A$  appears in a mixed state, with a reduced density matrix given by

$$\rho_A = \text{Tr}_{\bar{A}} \rho, \quad (4)$$

where  $\bar{A}$  is traced out. The information regarding the entanglement is encoded in  $\rho_A$ . As a result, the level of entanglement between  $A$  and  $\bar{A}$  is described by the entanglement entropy,

which is defined by

$$S_{\text{ent.}} = \text{Tr}_A[\rho_A \ln \rho_A]. \quad (5)$$

Since the vacuum wave-function of  $\bar{A}$  is buried in the excited wave-functions of the “mix-state” subsystem  $A$  described by  $\rho_A$ , the expectation value of a local operator can be computed by

$$\langle 0 | \mathcal{O}_A | 0 \rangle = \frac{\text{Tr}[\rho_A \mathcal{O}_A]}{\text{Tr}[\rho_A]}. \quad (6)$$

One example of such set-up is the black holes. Suppose that the whole spacetime is in a pure state, but we are unable to access the region inside the event horizon. Therefore the black hole appears thermal to an outside observer due to the entanglement between the two regions separated by the horizon, and so the entropy arise. This is one interpretation of the black hole entropy.

In this paper, we will consider the case that the system  $S$  contains the whole space, while the subsystems  $A$  and  $\bar{A}$  each occupies the infinite half-space, divided by a codimension 2 (with respect to the whole spacetime) surface. We follow the convention in [22], denoting the time  $t$  and radial coordinate  $x_{\parallel}$  as the *longitudinal directions*, as they are relevant in our field theory calculation, while the *transverse directions* indicate the dimensions of the surface enclosing the subsystem  $A$ .

In order to calculate the entanglement entropy, we take the generic scalar field theory as an example and review the replica method in the following. The entanglement entropy can be calculated by the following trick[17, 18, 22]

$$S_{\text{ent.}} = - \left. \frac{\partial}{\partial n} \right|_{n \rightarrow 1} \ln \text{Tr}[\rho_A^n] = -\text{Tr}[\rho_A \ln \rho_A], \quad (7)$$

where the trace is taken within  $A$  implicitly. As  $n \rightarrow 1$ , we can take  $n = 1 + \epsilon$  and expand  $\ln \text{Tr}[\rho_A^n]$  in  $\epsilon$  for small  $\epsilon$ . Then the entanglement entropy can be spelled out from the  $O(\epsilon)$  term.

To calculate (7), we first notice that the elements of the reduced density matrix  $\rho_A$  can be expressed in the path integral formalism,

$$\langle \varphi_A | \rho_A | \varphi'_A \rangle = \int \mathcal{D}\phi \delta[\phi_A(\tau = 0^+) - \varphi_A] \delta[\phi_A(\tau = 0^-) - \varphi'_A] e^{-S_E[\phi = \phi_A \oplus \phi_{\bar{A}}]}, \quad (8)$$

where  $S_E$  is the action of  $\phi$  over the whole Euclidean space with imaginary time  $\tau$ .  $\phi_A, \phi_{\bar{A}}$  are the scalar fields taking values in  $A, \bar{A}$  respectively. The field bases  $|\varphi_A\rangle$  and  $|\varphi'_A\rangle$  are



states in  $A$  at certain time. In this expression,  $\bar{A}$  region is traced out. Since taking trace amounts to identifying the Euclidean time of the initial and the final states, (8) implies that  $\rho_A$  is computed on a manifold where  $\bar{A}$  is compactified (in  $\tau$  direction) to a cylinder while  $A$  is left open. When we had identified  $\phi(\tau = -\infty) = \phi(\tau = \infty)$ , the matrix element of  $\rho_A^n$  is computed on a manifold on which  $\bar{A}$  consists of  $n$  cylinders on top of each other while  $A$  becomes a  $n$ -sheeted spacetime manifold. Taking trace of  $\rho_A^n$  then joins the first sheet with the last for  $A$ , compactifying it into a cone with a total angle  $2n\pi$  (or an excess angle  $\delta = 2(n-1)\pi$ ), where  $n \geq 1$ . See e.g. Fig. 1 in [22] or Fig.'s 1 and 2 in [18] for the pictorial realization. As a result, it is natural to define the trace of  $\rho_A^n$  by

$$\ln \text{Tr}[\rho_A^n] = \ln \left( \frac{Z_n}{Z_1^n} \right), \quad (9)$$

where  $Z_n$  denotes the partition function of the field theory on the  $n$ -sheet manifold. ( $n = 1$  reduces to the case on the ordinary Euclidean space.) The normalization by  $Z_1^n$  is due to the requirement that  $\text{Tr}[\rho_A^n]|_{n \rightarrow 1} = 1$ .

To summarize, using the replica trick, the entanglement entropy is calculated by

$$S_{\text{ent.}} = - \frac{\partial}{\partial n} [\ln Z_n - n \ln Z_1] \Big|_{n \rightarrow 1} = - \frac{1}{\epsilon} [\ln Z_n - n \ln Z_1]. \quad (10)$$

For  $n > 1$ , the replication of sheets takes place in the Euclidean time coordinate, which belong to the longitudinal directions, while the transverse directions remain ordinary Euclidean. We will adopt polar coordinates for the longitudinal part of the spacetime,

$$(\tau, x_{\parallel}) = (r \sin \frac{\theta}{n}, r \cos \frac{\theta}{n}), \quad (11)$$

where  $r \in (0, +\infty)$  and  $\theta$  is periodical with  $2\pi n$ . Thus the partition function on the  $n$ -sheet manifold is written down as

$$Z_n = \int \mathcal{D}\phi \exp \left[ - \int d^{d+1}x_{\perp} \int_0^{\infty} r dr \int_0^{2\pi n} d\theta \mathcal{L}_{\text{E}}[\phi(r, \theta, x_{\perp})] \right]. \quad (12)$$

Such expression is valid only for the total spacetime dimensions  $d + 1 > 2$ .

Since the partition function in quantum field theory is interpreted as the vacuum energy, and the entanglement entropy of our model is obtained by (10),  $S_{\text{ent.}}$  can be interpreted as the derivative of the correction to the vacuum energy due to the cone with respect to the conical deficit angle. This notion will be more transparent as we calculate the free field entanglement entropy in the  $O(N)$  symmetric phase in next section.

### III. PERTURBATION EXPANSION OF THE $O(N)$ $\sigma$ -MODEL IN THE SYMMETRIC PHASE

The Euclidean Lagrangian of  $3 + 1$  dimensional  $O(N)$  model is given by

$$\mathcal{L}_E = \sum_{i=1}^N \left[ \frac{1}{2} (\partial \phi^i)^2 + \frac{1}{2} \mu^2 (\phi^i)^2 \right] + \frac{\lambda}{4} \left[ \sum_{i=1}^N (\phi^i)^2 \right]^2 + \mathcal{L}_{c.t.}, \quad (13)$$

which has  $N$  species of scalar fields with the same mass  $\mu$ , admitting  $O(N)$  symmetry and quartic interactions.  $\mathcal{L}_{c.t.}$  is the counter terms to cancel the loop corrections.

Since in this paper we use the renormalized mass  $\mu$  and the renormalized coupling constant  $\lambda$  in the tree level action, the partition function on  $n$ -sheet manifold can be expanded with respect to  $\lambda$  by

$$\ln Z_n = \ln Z_{n,0} + \sum_{j=1}^{\infty} \frac{(-\lambda)^j}{4^j j!} \int \left( \prod_{k=1}^j d^{d_{\perp}} x_{k\perp} \right) \int_n \left( \prod_{k=1}^j d^2 x_{k\parallel} \right) \left\{ \left\langle \left[ \sum_{m=1}^N \phi^m(x_1)^2 \right]^2 \dots \left[ \sum_{n=1}^N \phi^n(x_j)^2 \right]^2 \right\rangle_0 + \text{counter terms} \right\}, \quad (14)$$

where  $\ln Z_{n,0}$  denotes the  $O(\lambda^0)$  free field part. The counter terms are introduced to cancel the divergence from the perturbative corrections of loops, such that the renormalized  $\mu$  and  $\lambda$  receives no further quantum corrections.  $\int_n$  is the integral over the 2-dimensional  $n$ -sheet manifold  $\int_0^\infty r dr \int_0^{2\pi n} d\theta$ .

In the following we calculate the entanglement entropy up to lowest-order corrections (in this case,  $O(\lambda)$  bubble diagrams). The free field contribution is computed by the following method[22]. First, one notices that

$$\frac{\partial}{\partial \mu^2} \ln Z_{n,0} = -\frac{1}{2} \int_n d^{d+1}x G_n(x, x), \quad (15)$$

where  $G_n(x, x')$  is the Green's function of the free scalars on the  $n$ -sheet Riemann surface, satisfying  $(-\nabla^2 + \mu^2) G_n(x, x') = \delta^{d+1}(x - x')$ . The expression for the Green's function on  $n$ -sheet Riemann surface  $G_n(x, x')$  is very complicated, see [31] for details. (We will use it later in (32) in the broken phase.) However, if  $x'$  coincides with  $x$ , however, the Green's function becomes relatively simpler and we employ an approximation used in [17] and [22].  $G_n(x, x)$  can be decomposed into

$$G_n(x, x) = G_1(0) + f_n(r). \quad (16)$$

$G_1(0) = G_1(|x - x|)$  is the (divergent) Green's function on the Euclidean flat space, which admits translational invariance, and  $f_n(r)$  represents the correction to the one-loop vacuum bubble due to the conical singularity [22]:

$$\begin{aligned} f_n(r) &= \frac{1}{2\pi n} \frac{1-n^2}{6n} \int \frac{d^{d_\perp} p_\perp}{(2\pi)^{d_\perp}} K_0^2(\sqrt{\mu^2 + p_\perp^2} r) + \dots \\ &\stackrel{n=1+\epsilon}{=} -\frac{\epsilon}{6\pi} \int \frac{d^{d_\perp} p_\perp}{(2\pi)^{d_\perp}} K_0^2(\sqrt{\mu^2 + p_\perp^2} r) + O(\epsilon^2) + \dots, \end{aligned} \quad (17)$$

with

$$\int_0^\infty dy y K_0^2(y) = \frac{1}{2} \quad \Rightarrow \quad \int_0^\infty r dr K_0^2(\sqrt{\mu^2 + p_\perp^2} r) = \frac{1}{2} \frac{1}{\mu^2 + p_\perp^2}, \quad (18)$$

where  $K_0$  is the modified Bessel function of the second kind  $K_\nu$  with  $\nu = 0$ , and  $\dots$  denotes the finite subleading terms. Since  $f_n$  is finite for  $r > 0$  and decays exponentially at  $r \rightarrow \infty$  (see Fig. 1), one can see that  $f_n$  vanishes for  $n \rightarrow 1$  (i.e.  $\epsilon \rightarrow 0$ , where  $\epsilon = n - 1$  is the deficit angle of the cone), as expected.

Now we can make use of (15) and the subsequent approximation of  $G_n(x, x)$  in (17) and (18) to calculate the free fields contribution to the entanglement entropy in the  $O(N)$  symmetric phase from (10):

$$\begin{aligned} S_{\text{ent.}}^{\text{free}}(\mu^2) &= -\frac{1}{\epsilon} (\ln Z_{1+\epsilon,0} - (1+\epsilon) \ln Z_{1,0}) \\ &= \frac{N}{\epsilon} \int_\infty^{\mu^2} \frac{dm^2}{2} \int d^{d_\perp} x_\perp \left\{ \int_{1+\epsilon} d^2 x_\parallel G_n(x, x) - (1+\epsilon) \int_1 d^2 x_\parallel G_1(x, x) \right\}. \end{aligned}$$

The reason for integrating the mass squared parameter from  $\infty$  to  $\mu^2$  is because we expect the entanglement entropy to vanish at  $\mu^2 = \infty$ , due to vanishing correlation length  $\xi \sim \mu^{-1}$ .

We can further decompose the integration range into  $\int_\infty^{\mu^2} dm^2 = \left( \int_\infty^0 + \int_0^{\mu^2} \right) dm^2$ ,

$$\begin{aligned} S_{\text{ent.}}^{\text{free}}(\mu^2) &= \frac{N}{\epsilon} \left( \int_\infty^0 + \int_0^{\mu^2} \right) \frac{dm^2}{2} \int d^{d_\perp} x_\perp \int_{1+\epsilon} d^2 x_\parallel f_{1+\epsilon}(r) \\ &= -A_\perp \frac{N}{12} \int \frac{d^{d_\perp} p_\perp}{(2\pi)^{d_\perp}} \left[ \int_\infty^0 \frac{dm^2}{m^2 + p_\perp^2} + \int_0^{\mu^2} \frac{dm^2}{m^2 + p_\perp^2} \right] \\ &= -A_\perp \frac{N}{12} \int \frac{d^{d_\perp} p_\perp}{(2\pi)^{d_\perp}} \left[ \ln \frac{p_\perp^2}{\Lambda^2 + p_\perp^2} + \ln \frac{\mu^2 + p_\perp^2}{p_\perp^2} \right] \\ &= -A_\perp \frac{N}{12} \int \frac{d^{d_\perp} p_\perp}{(2\pi)^{d_\perp}} \ln \frac{\mu^2 + p_\perp^2}{\Lambda^2 + p_\perp^2}, \end{aligned} \quad (19) \quad (20)$$

where  $A_\perp = \int d^{d_\perp} x_\perp$  is the total area of the transverse space separating  $A$  and  $\bar{A}$ , and  $\Lambda$  is the mass scale (or momentum) cutoff in the integration over  $dm^2$ . In the above calculation,  $\int_n d^2 x_\parallel G_1(0)$  and  $n \int_1 d^2 x_\parallel G_1(0)$  cancel out exactly.

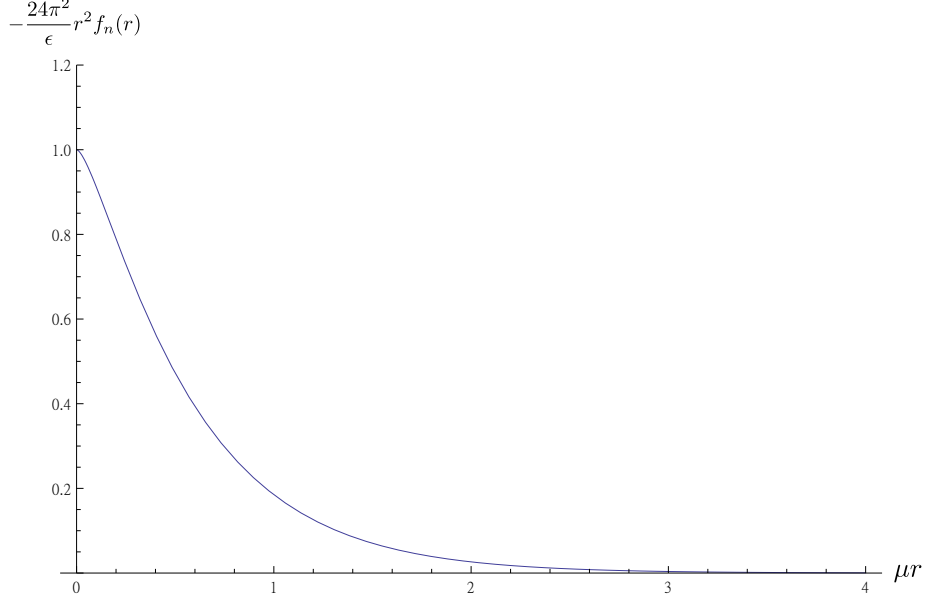


Figure 1. Behavior of  $f_n(r)$ , giving rise to the subleading divergence in  $S_{\text{ent.}}^{\text{free}}(\mu^2)$ .

In (20), the leading divergence  $\sim \Lambda^{d-1}$  comes from  $\int_{\infty}^0 \frac{dm^2}{2} \int d^{d_{\perp}} x_{\perp} \int_{1+\epsilon} d^2 x_{\parallel} f_{1+\epsilon}(r)$ . This can be seen from the  $(K_0)^2$  integral in (17) in 3+1 dimensions ( $d = 3$ ):

$$\frac{1}{\epsilon} r^2 f_n(r) \sim - \int dp_{\perp} p_{\perp} K_0^2(\sqrt{\mu^2 + p_{\perp}^2} r) = \frac{\mu^2}{2} (K_0(\mu r)^2 - K_1(\mu r)^2) \quad (21)$$

$$\sim \begin{cases} -\frac{1}{2} + \frac{(\mu r)^2}{2} [(\ln \mu r)^2 + \dots] + O(\mu^3 r^3), & r \rightarrow 0 \\ -e^{2\mu r}, & r \rightarrow \infty \end{cases} \quad (22)$$

as displayed in Fig. 1. Such behavior means, as the location of the quantum bubble is far away from the tip of the cone, the effect of the conical singularity is exponentially suppressed, and the bubble sees a flat Euclidean space. While the quantum bubble is very close to the conical point, it is  $\frac{1}{r^2}$  divergent. Then plug (21) into (19), one finds that

$$\begin{aligned} S_{\text{ent.}}^{\text{free}} \Big|_{\text{leading}} &\sim \int r dr \int_{\infty}^0 dm^2 \frac{m^2}{2} (K_0(\mu r)^2 - K_1(\mu r)^2) \\ &= \int r dr \frac{-1}{3r^4} \propto \Lambda^2. \end{aligned} \quad (23)$$

On the other hand, the subleading contribution  $\sim \ln \Lambda$  to the entanglement entropy comes from the integral  $\int_0^{\mu^2} \frac{dm^2}{2} \int d^{d_{\perp}} x_{\perp} \int_{1+\epsilon} d^2 x_{\parallel} f_{1+\epsilon}(r)$ . It is straightforward to check by substituting the leading term in (22) at small  $r$  into (19), and then going through the calculation in (23).

Since the calculation of  $S_{\text{ent.}}^{\text{free}}$  in (19) stems from (10), where  $f_n$  is the correction to the one-loop vacuum bubble due to the cone, it would be more clear here to comprehend the

interpretation of the entanglement entropy as the derivative of the correction to the vacuum energy due to the cone with respect to the conical deficit angle, as mentioned in the end of the previous section.

The perturbation at  $O(\lambda)$  level contributes to the partition function by

$$\begin{aligned}\ln Z_{n,1} &= -\frac{\lambda}{4} \int d^{d_\perp} x_\perp \int_n d^2 x_\parallel \langle \left[ \sum_{i=1}^N \phi^i(x)^2 \right]^2 \rangle_0 \\ &= -\frac{\lambda}{4} \int d^{d_\perp} x_\perp \int_n d^2 x_\parallel (N^2 + 2N) [G_n(x, x)^2],\end{aligned}\quad (24)$$

where we had used  $G_n^{ij}(x, x') = \delta^{ij} G_n(x, x')$ . Then we get

$$\begin{aligned}S_{\text{ent.}}(\mu^2, O(\lambda)) &= \frac{1}{\epsilon} \frac{\lambda}{4} (N^2 + 2N) \int d^{d_\perp} x_\perp \left[ \int_{1+\epsilon} d^2 x_\parallel G_{1+\epsilon}(x, x)^2 - (1 + \epsilon) \int d^2 x_\parallel G_1(x, x)^2 \right] \\ &= -\frac{N}{12} \lambda (N^2 + 2N) G_1(0) A_\perp \int \frac{d^{d_\perp} p_\perp}{(2\pi)^{d_\perp}} \frac{1}{\mu^2 + p_\perp^2},\end{aligned}\quad (25)$$

in which we have used (16)~(18), and as a result  $\int_n G_1^2$  is canceled out by  $n \int G_1^2$ , leaving  $\int_n G_1(0) f_n(r)$  as the leading contribution  $O(\epsilon)$  in  $\epsilon$ .

The following counter term is introduced to cancel the above  $O(\lambda)$  corrections:

$$-\frac{1}{2} \delta \mu^2 \sum_{i=1}^N (\phi^i)^2, \quad (26)$$

where

$$\delta \mu^2 = -(N + 2) \lambda G_1(0). \quad (27)$$

This implies the renormalized mass  $\mu$  is related to the bare mass  $\mu_b$  by  $\mu^2 = \mu_b^2 + (N + 2) \lambda G_1(0)$ . This result is consistent with [22]. The derivation of (27) is summarized in Appendix for the interested readers. As a result, the entanglement entropy of the  $\sigma$ -model in the  $O(N)$  symmetric phase is given by (20).

In 3+1 dimensions,  $d_\perp = 2$ , (20) gives rise to the following divergence structure:

$$S_{\text{ent}}(\mu^2, \lambda) = \frac{A_\perp^{(2)} \Lambda^2}{48\pi} N \left\{ \ln 4 + \left( \frac{\mu^2}{\Lambda^2} \right) \ln \left( \frac{\mu^2}{\Lambda^2} \right) + O \left( \tilde{\lambda}^2, \frac{\mu^2}{\Lambda^2} \right) \right\}, \quad (28)$$

where  $A_\perp$  is the area of a 2-dimensional boundary surface of  $A$ . All the correction at  $O(\lambda)$  are canceled by the counter terms.

#### IV. $O(N)$ $\sigma$ -MODEL IN THE SYMMETRY BROKEN PHASE

The spontaneous symmetry breaking of  $O(N)$  occurs when the mass squared of the scalar fields  $\phi^i$  is tuned to  $\mu^2 < 0$ . Let's suppose the SSB occurs in the  $\phi^N$  direction, i.e.  $\phi^N$  develops a VEV  $v$ . Then the system is left with  $N - 1$  massless Goldstone bosons  $\pi^1, \dots, \pi^{N-1}$  and 1 massive scalar  $\sigma$ ,

$$(\phi^1, \phi^2, \dots, \phi^{N-1}, \phi^N) = (0, 0, \dots, 0, v) + (\pi^1, \pi^2, \dots, \pi^{N-1}, \sigma), \quad (29)$$

where the condensate  $v$  takes the value

$$v = \langle \phi^N \rangle = \frac{m_\sigma}{\sqrt{2}g}, \quad (30)$$

with  $m_\sigma = \sqrt{-2\mu^2}$  and the new coupling constant  $g = \sqrt{\lambda}$ . The Euclidean Lagrangian in the SSB phase becomes

$$\begin{aligned} \mathcal{L}_E = & \sum_{i=1}^{N-1} \frac{1}{2} (\partial \pi^i)^2 + \frac{1}{2} (\partial \sigma)^2 + \frac{1}{2} m_\sigma^2 \sigma^2 \\ & + \frac{g}{\sqrt{2}} m_\sigma \left( \sum_{i=1}^{N-1} (\pi^i)^2 \sigma + \sigma^3 \right) + \frac{g^2}{4} \left( \left[ \sum_{i=1}^{N-1} (\pi^i)^2 \right]^2 + \sigma^4 + 2 \sum_{i=1}^{N-1} (\pi^i)^2 \sigma^2 \right). \end{aligned} \quad (31)$$

Compared to the original  $O(N)$   $\sigma$ -model, the SSB phase contains not only the quartic interactions but also the cubic ones with coupling  $gm_\sigma/\sqrt{2}$ .

Since we use the renormalized  $g$  and  $m_\sigma$  in the action, it requires to add counter terms to the classical action to cancel the loop effects, The partition function up to  $O(g^2)$  corrections

with respect to the new coupling constant  $g$  and  $m_\sigma$  becomes,

$$\begin{aligned}
\ln Z_n^{\text{SSB}} &= \ln Z_{n,0}^{\text{SSB}} - \frac{g^2}{4} \int d^{d_\perp} x_\perp \int_n d^2 x_\parallel \left\{ \left\langle \left[ \sum_{i=1}^{N-1} (\pi^i)^2 \right]^2 \right\rangle + \langle \sigma^4 \rangle + 2 \sum_{i=1}^{N-1} \langle (\pi^i)^2 \sigma^2 \rangle \right\} \\
&\quad + \frac{g^2}{4} m_\sigma^2 \int d^{d_\perp} x_\perp d^{d_\perp} x'_\perp \int_n d^2 x_\parallel d^2 x'_\parallel \left\{ \langle \sigma^3(x) \sigma^3(x') \rangle \right. \\
&\quad \left. + \sum_{i,j=1}^{N-1} \langle [\pi^i(x)]^2 \sigma(x) [\pi^j(x')]^2 \sigma(x') \rangle + 2 \sum_{i=1}^{N-1} \langle [\pi^i(x)]^2 \sigma(x) \sigma^3(x') \rangle \right\} \\
&\quad + \text{integral of counter terms} \\
&= \ln Z_{n,0}^{\text{SSB}} \\
&\quad - \frac{g^2}{4} \int_n d^{d+1} x \left[ (N^2 - 1) G_n^\pi(x, x)^2 + 3 G_n^\sigma(x, x)^2 + 2(N - 1) G_n^\pi(x, x) G_n^\sigma(x, x) \right] \\
&\quad + \frac{g^2}{4} m_\sigma^2 \int d^{d_\perp} x_\perp d^{d_\perp} x'_\perp \int_n d^2 x_\parallel d^2 x'_\parallel \left[ 6 G_n^\sigma(x', x)^3 + 2(N - 1) G_n^\pi(x', x)^2 G_n^\sigma(x', x) \right] \\
&\quad + \text{integral of counter terms.} \tag{32}
\end{aligned}$$

This is up to  $O(g^2) \sim O(\lambda)$ .  $\ln Z_1^{\text{SSB}}$  can also be obtained analogously. Note that the expectation value here is taken with respect to the new vacuum in the symmetry broken phase. In terms of Feynman diagrams, these  $O(g^2) \sim O(\lambda)$  terms in the second and the third lines of (32) are depicted by the one-vertex and two-vertex two-loops in Fig. 2 respectively.

The counter terms added to the action for canceling the two-loop contributions are

$$-\frac{g^2}{2} \left( \delta^{(1)} \mu^2 + \frac{m_\sigma^2}{2} \delta^{(2)} \lambda \right) \sum_{i=1}^{N-1} (\pi^{i2})^2 - \frac{g^2}{2} \left( \delta^{(1)} \mu^2 + \frac{3m_\sigma^2}{2} \delta^{(2)} \lambda \right) \sigma^2 - \frac{gm_\sigma}{\sqrt{2}} \left( \delta^{(1)} \mu^2 + \frac{m_\sigma^2}{2} \delta^{(2)} \lambda \right) \sigma, \tag{33}$$

where  $\delta^{(1)} \mu^2$ ,  $\delta^{(2)} \lambda$  denote the coefficients of the mass and the coupling constant renormalization counter terms respectively, with the superscripts (1), (2) labeling the orders in  $\lambda$  (see (52) in the Appendix for the meaning of the superscripts (1), (2)). Note that the wave function renormalization counter term does not involve up to  $O(\lambda)$  here.

In (32), we omit the cubic interactions  $\langle \pi^i(x) \pi^i(x) \sigma(x) \rangle$  and  $\langle \sigma(x) \sigma(x) \sigma(x) \rangle$  at  $O(g)$  level, because they both vanish. Moreover, the tadpole diagrams

$$\begin{aligned}
&\frac{g^2 m_\sigma^2}{4} \int_n d^{d+1} x \int_n d^{d+1} x' \left\{ 9 G_n^\sigma(x', x') G_n^\sigma(x', x) G_n^\sigma(x, x) \right. \\
&\quad \left. + (N - 1)^2 G_n^\pi(x', x') G_n^\sigma(x', x) G_n^\pi(x, x) + 6(N - 1) G_n^\pi(x', x') G_n^\sigma(x', x) G_n^\sigma(x, x) \right\}
\end{aligned} \tag{34}$$

are also dropped out, due to the requirement of the vanishing one-point function  $\langle \sigma \rangle = 0$  in the vacuum of broken phase such that these tadpole corrections to the one-point function

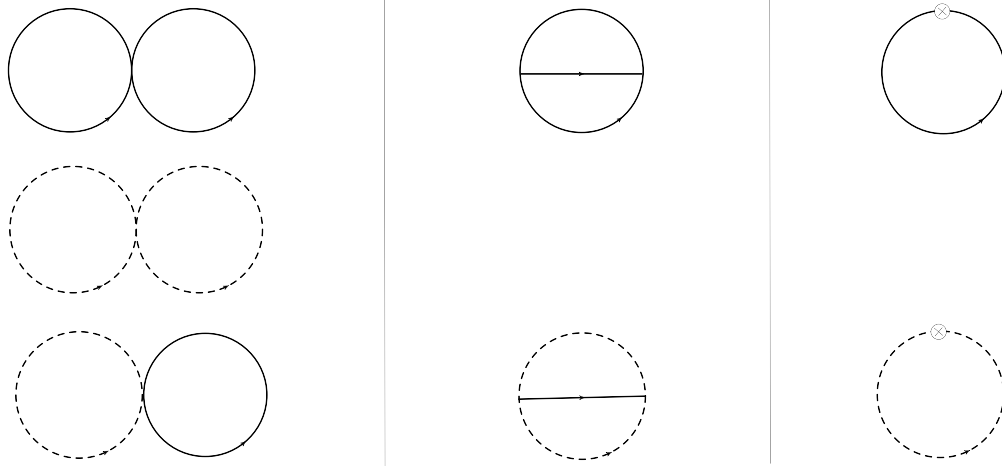


Figure 2. Feynman diagrams contributing to the two-loop corrections to the entanglement entropy in (32). The solid lines denote the massive mode  $\sigma$  while the dashed lines represent the Goldstone bosons  $\pi^i$ . The left column depicts the quartic interaction between  $\sigma$ 's and  $\pi^i$ 's. The middle column is the two-loops arising from the cubic interactions, while the right one represent the counter terms' effects to cancel the divergence due to the diagrams in the left and central column.

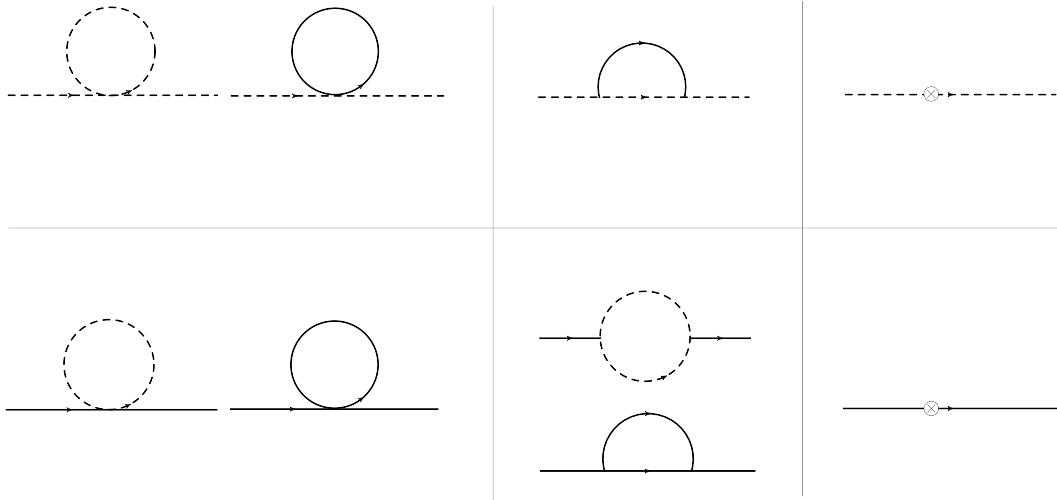


Figure 3. Feynman diagrams for the mass renormalization of  $\pi^i$ 's (the upper row) and  $\sigma$  (the lower row). The left column represents the contribution from the quartic interactions, while the middle one from the cubic interactions. The right column stands for the counter terms. The solid lines denote  $\sigma$  while the dashed lines  $\pi^i$ 's.



$\langle \sigma \rangle$  should be canceled out by the counter terms. This gets rid of the contribution from (34), and gives rise to the condition

$$\delta^{(1)}\mu^2 + \frac{m_\sigma^2}{2}\delta^{(2)}\lambda = -3G_\sigma(0) - (N-1)G_\pi(0). \quad (35)$$

The Feynman diagrams of the non-vanishing two-loop contributions are displayed in Fig. 3. The explicit expressions of the counter terms are given by

$$\begin{aligned} \delta^{(2)}\lambda &= 9L_\sigma(p^2 = m_\sigma^2) + (N-1)L_\pi(p^2 = m_\sigma^2), \\ \delta^{(1)}\mu^2 &= -3G_\sigma(0) - (N-1)G_\pi(0) - \frac{9m_\sigma^2}{2}L_\sigma(p^2 = m_\sigma^2) - \frac{m_\sigma^2}{2}(N-1)L_\pi(p^2 = m_\sigma^2), \end{aligned} \quad (36)$$

where  $L_{\pi,\sigma}(p^2)$  is defined as

$$L_{\pi,\sigma}(p^2) = \int \frac{d^{d+1}q}{(2\pi)^{d+1}} G_{\pi,\sigma}(p-q) G_{\pi,\sigma}(q). \quad (37)$$

We can now use (10) to calculate the entanglement entropy. The free field contribution is

$$S_{\text{ent.}}^{\text{SSB}(\text{free})}(m_\sigma^2) = -\frac{N-1}{12}A_\perp \int \frac{d^{d_\perp}p_\perp}{(2\pi)^{d_\perp}} \ln \frac{p_\perp^2}{\Lambda^2 + p_\perp^2} - \frac{1}{12}A_\perp \int \frac{d^{d_\perp}p_\perp}{(2\pi)^{d_\perp}} \ln \frac{m_\sigma^2 + p_\perp^2}{\Lambda^2 + p_\perp^2}. \quad (38)$$

The first term on the RHS is due to the (massless) Goldstone bosons  $\pi^1, \dots, \pi^{N-1}$ . The second term is from the massive scalar  $\sigma$ .

The two-loop corrections to the entanglement entropy are obtained as follows. The one-vertex sector (i.e. the second line in (32), or the left column of Fig. 2) is computed analogously to (25), and the result is

$$\begin{aligned} \Delta S_{\text{ent}(\text{1-vt})}^{\text{SSB}}(m_\sigma^2, g^2) &= -A_\perp \frac{g^2}{12} \left\{ \left( 3G_1^\sigma(0) + (N-1)G_1^\pi(0) \right) \int \frac{d^{d_\perp}p_\perp}{(2\pi)^{d_\perp}} \frac{1}{m_\sigma^2 + p_\perp^2} \right. \\ &\quad \left. + \left( (N-1)G_1^\sigma(0) + (N^2-1)G_1^\pi(0) \right) \int \frac{d^{d_\perp}p_\perp}{(2\pi)^{d_\perp}} \frac{1}{p_\perp^2} \right\}. \end{aligned} \quad (39)$$

As for the two-vertex sector (i.e. the third line in (32), or the middle column in Fig. 2), in general the Green's function on  $n$ -sheet Riemann surface  $G_n(x, x')$  is very complicated. [22] proposes some approximation to simplify the calculation, but we discover that part of [22]'s approximation is invalid, as explained below. Then we will adopt the approach used in [31] instead in our calculation. The Green's function  $G_n(x, x')$  on the cone can be decompose into

$$G_n(x, x') = G_1(|x - x'|) + f_n(x, x'), \quad (40)$$

where  $G_1$  represents the  $O(\epsilon^0)$  part while  $f_n$  the  $O(\epsilon)$  (and the higher order) effects of the Green's function, in analogy to (16), and  $\epsilon$  is the deficit angle of the cone. It is noticed that  $\int_n d^{d+1}x \int_n d^{d+1}x' G_1(|x - x'|)^3 - n \int_1 d^{d+1}x \int_1 d^{d+1}x' G_1(|x - x'|)^3$  is subleading at UV, where  $G_1(|x - x'|)$  could either denotes the Green's function for  $\sigma$  or  $\pi^i$ . For convenience we change the coordinates from  $(x, x')$  to  $(x, y)$  with  $y = x' - x$ , such that the aforementioned subtraction becomes

$$\int_n d^{d+1}x \int_n d^{d+1}y G_1(|y|)^3 - n \int_1 d^{d+1}x \int_1 d^{d+1}y G_1(|y|)^3. \quad (41)$$

[22] argues that the divergence of  $G_1(|y|)$  occurs at small  $y \sim \Lambda^{-1}$ , i.e. as  $x'$  approaches  $x$ , where the fields at  $x'$  couldn't "sense" the existence of the conical point when  $x$  is not close to the conical singularity. This means that for the divergent part of  $G_1(|y|)$ , the integration over  $\int_n d^{d+1}y$  actually takes  $2\pi$  angle for  $y$  to encircle  $x$  once instead of taking  $2n\pi$ , and hence contributes no  $n$  factor. The only  $n$  factor in the first term of (41) is from  $\int_n d^{d+1}x$ . Then it is straightforward to see that, at UV, (41) schematically behaves as

$$nV\Lambda^{d-1} - nV\Lambda^{d-1},$$

and the two terms cancel out.

However, we notice that this argument breaks down when  $x$  is very close to the conical singularity, i.e.  $|x| < \Lambda^{-1}$ , such that the conical singularity is located within  $y < \Lambda^{-1}$ . In this case, both  $\int_n d^{d+1}x$  and  $\int_n d^{d+1}y$  give rise to an  $n$  factor, but the former only produce a  $A_\perp 2n\pi/\Lambda^2$  coefficient due to restricting  $|x| < \Lambda^{-1}$ . So in this scenario, (41) has non-vanishing but finite contribution proportional to

$$A_\perp \frac{n^2}{\Lambda^2} \Lambda^{d-1} - A_\perp \frac{n}{\Lambda^2} \Lambda^{d-1} = A_\perp \Lambda^{d-3} (n^2 - n),$$

whose contribution is of higher order in the entanglement entropy.

In terms of  $(x, y)$  coordinates, the leading divergent contribution to  $\Delta S_{\text{ent}(2\text{-vt})}^{\text{SSB}}(g^2)$  comes from

$$\begin{aligned} \frac{g^2 m_\sigma^2}{4} \int_n d^{d+1}x \int_n d^{d+1}y \left\{ 18 G_1^\sigma(|y|)^2 f_n^\sigma(x, y) \right. \\ \left. + 2(N-1) \left[ 2 G_1^\sigma(|y|) G_1^\pi(|y|) f_n^\pi(x, y) + G_1^\pi(|y|)^2 f_n^\sigma(x, y) \right] \right\}. \end{aligned} \quad (42)$$

By further decomposing  $y$  into  $y_\perp$  and  $y_\parallel$ , the above expression gives rise to the following

corrections to the entanglement entropy:

$$\Delta S_{\text{ent}(2\text{-vt})}^{\text{SSB}}(m_\sigma^2, g^2) \sim \frac{g^2 A_\perp}{12} \int \frac{d^{d_\perp} p_\perp}{(2\pi)^{d_\perp}} \frac{m_\sigma^2}{m_\sigma^2 + p_\perp^2} \times [9\Gamma_\sigma(p_\perp^2) + (N-1)\Gamma_\pi(p_\perp^2) + 2(N-1)\Gamma_{\pi\sigma}(p_\perp^2)], \quad (43)$$

where

$$\begin{aligned} \Gamma_{\pi\sigma}(p_\perp^2) &= \int \frac{d^2 k_\parallel}{(2\pi)^2} \frac{d^2 k_\perp}{(2\pi)^2} \frac{1}{k^2 + m_\sigma^2} \frac{1}{k_\parallel^2 + (\mathbf{k}_\perp + \mathbf{p}_\perp)^2}, \\ \Gamma_\pi(p_\perp^2) &= \int \frac{d^2 k_\parallel}{(2\pi)^2} \frac{d^2 k_\perp}{(2\pi)^2} \frac{1}{k^2} \frac{1}{k_\parallel^2 + (\mathbf{k}_\perp + \mathbf{p}_\perp)^2}, \\ \Gamma_\sigma(p_\perp^2) &= \int \frac{d^2 k_\parallel}{(2\pi)^2} \frac{d^2 k_\perp}{(2\pi)^2} \frac{1}{k^2 + m_\sigma^2} \frac{1}{k_\parallel^2 + (\mathbf{k}_\perp + \mathbf{p}_\perp)^2 + m_\sigma^2}. \end{aligned} \quad (44)$$

These three expressions correspond to the three one-loop Feynman diagrams from the top to the bottom in the middle column of Fig. 3 respectively.

One expects that two-loop contributions from (39) and (43) will be canceled by the counter terms in (33). This is indeed the case for the one-vertex sector (39); however there are residual terms from (43) after the cancellation,

$$\begin{aligned} \Delta S_{\text{ent}(\text{res})}^{\text{SSB}}(m_\sigma^2, g^2) &\sim g^2 \frac{A_\perp}{12} \int \frac{d^2 p_\perp}{(2\pi)^2} \frac{m_\sigma^2}{p_\perp^2 + m_\sigma^2} [9D_\sigma(p_\perp^2, q^2) + (N-1)D_\pi(p_\perp^2, q^2)]|_{q^2=m_\sigma^2} \\ &+ g^2 \frac{(N-1)A_\perp}{12} \int \frac{d^2 p_\perp}{(2\pi)^2} \frac{m_\sigma^2}{p_\perp^2 + m_\sigma^2} [2D_{\pi\sigma}(p_\perp^2, q^2)]|_{q^2=0}, \end{aligned} \quad (45)$$

where

$$\begin{aligned} D_\sigma(p_\perp^2, q^2) &= \Gamma_\sigma(p_\perp^2) - L_\sigma(q^2) \neq 0, \\ D_\pi(p_\perp^2, q^2) &= \Gamma_\pi(p_\perp^2) - L_\pi(q^2) \neq 0, \\ D_{\pi\sigma}(p_\perp^2, q^2) &= \Gamma_{\pi\sigma}(p_\perp^2) - L_{\pi\sigma}(q^2) \neq 0, \end{aligned} \quad (46)$$

with  $L_\sigma, L_\pi$  and  $L_{\pi\sigma}$  given by (37).

The existence of these cancellation remnants means that the expansion of  $S_{\text{ent.}}^{\text{SSB}}$  involves non-trivial subleading terms. In 3+1 dimensions, the entanglement entropy reads

$$\begin{aligned} S_{\text{ent.}}^{\text{SSB}}(m_\sigma^2, \lambda) &= \frac{1}{48\pi} N A_\perp \Lambda^2 \left[ \ln 4 - \frac{\frac{3}{2}N + 3}{(4\pi N)^2} \tilde{\lambda} \left( \frac{m_\sigma^2}{\Lambda^2} \right) \left[ \ln \left( \frac{m_\sigma^2}{\Lambda^2} \right) \right]^2 \right. \\ &\quad \left. + \left( \frac{1}{N} - \frac{2(N-1) + 9\sqrt{5} \ln((3+\sqrt{5})/2)}{(4\pi N)^2} \tilde{\lambda} \right) \left( \frac{m_\sigma^2}{\Lambda^2} \right) \ln \left( \frac{m_\sigma^2}{\Lambda^2} \right) + O \left( \tilde{\lambda}^2, \frac{m_\sigma^2}{\Lambda^2} \right) \right]. \end{aligned} \quad (47)$$

The calculation detail for obtaining (47) from (42) is presented in the Appendix. The  $\lambda$ -independent part represents the exact cancellation between the quantum corrections and

the counter term of the quartic sector, leaving only the tree level effects, as in the  $O(N)$  symmetric phase. In this part, the leading divergence remains the same compared to the symmetric phase, contributed from  $N - 1$   $\pi$ 's and one  $\sigma$ , while the  $N$ -independent log divergence arises solely from  $\sigma$ , since it is the only massive component in the broken phase. The  $\lambda$ -dependent part in (47) represents the leftover of the cancellation between the two-vertex two-loop sector (due to the cubic interactions) and the counter terms, giving rise to the log squared divergence in the subleading part, which is more divergent than the subleading log divergence in (28) in the  $O(N)$  symmetric phase.

We emphasize that the highest subleading divergence of the entanglement entropy we obtained in (47) is log squared in the broken phase. This is different from the single log result of cubic interaction in [22]. The reason is as follows. The author in [22] argues that the leading divergence of (42) is contributed by  $y \rightarrow 0$ , i.e. both  $y_\perp \rightarrow 0$  and  $y_\parallel \rightarrow 0$ , such that  $f_n(x, y)$  becomes (17), and eventually (42) gives rise to a log divergence as the subleading behavior of entanglement entropy. But our calculation shows that  $y \neq 0$  part in  $f_n(x, y)$  is actually more divergent than log, and yields the log squared term, by setting  $y_\parallel \rightarrow 0$  (which allows  $f_n(x, y)$  to be approximated by (17)) while preserving the  $y_\perp \neq 0$  contribution and carrying out the Fourier transformation.

## V. NUMERICAL RESULTS OF ENTANGLEMENT ENTROPY

In this section, we present how the entanglement entropy varies with mass and how it behaves upon quantum phase transition in the  $O(N)$   $\sigma$ -model, up to  $O(\lambda)$ . This result is obtained by the numerical computation.

The numerical value of the entanglement entropy normalized by  $A_\perp \Lambda^2 N$  against  $\mu^2/\Lambda^2$  in both phases are plotted in Fig. 4. The  $\mu^2 > 0$  and  $\mu^2 < 0$  regions are the  $O(N)$  symmetric phase and the broken phase, respectively. This plot is shown in terms of renormalized  $\mu^2$ , with  $\tilde{\lambda}$  set to  $10^{-6}$ . In the  $O(N)$  symmetric phase, the leading and subleading parts of  $S_{\text{ent}}$  solely arise from the free fields, and is  $\lambda$ -independent. On the other hand, in the symmetry broken phase,  $S_{\text{ent}}^{\text{SSB}}$  contains the free field contribution and the  $\lambda$ -dependent remnant from counter terms cancellation of two-loop corrections due to the cubic interactions. The latter is shown in Fig. 5.

At the quantum critical point at  $\mu^2 = 0$ , one expects that the system acquires scaling

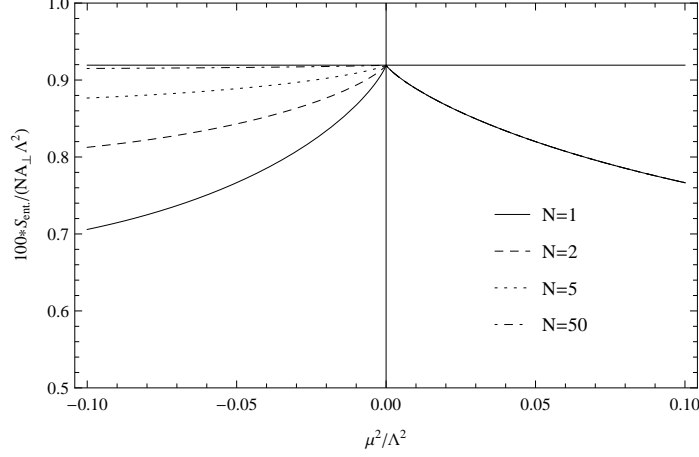


Figure 4. Entanglement entropy of the  $O(N)$   $\sigma$ -model in 3+1 dimensions, in units of  $NA_{\perp}\Lambda^2$  magnified by a factor of 100, against the mass squared of fields  $\mu^2$  normalized by  $\Lambda^2$ . The left half ( $\mu^2 < 0$ , with  $m_{\sigma}^2 = -2\mu^2$ ) is the spontaneous symmetry broken phase while the right half ( $\mu^2 > 0$ ) is the symmetric phase. In this plot, we take  $\tilde{\lambda} = 10^{-6}$  in order for the perturbation calculation to be valid. There is a cusped finite maximum at the quantum phase transition point  $\mu^2/\Lambda^2 = 0$ .

symmetry, which gives rise to universal properties, including the scaling law of the order parameters. For the entanglement entropy up to the highest subleading term, we found a novel scaling behavior near the transition point:

$$S_{\text{ent}} \sim \begin{cases} 1 + \frac{1}{\Lambda^2 \ln 4} \mu^2 \ln \mu^2 = (\mu^2)^{\frac{\mu^2}{\Lambda^2 \ln 4}} & \text{(symmetric phase)} \\ 1 - \alpha m_{\sigma}^2 \left( \ln m_{\sigma}^2 \right)^2 = \left( m_{\sigma}^2 \right)^{-\alpha m_{\sigma}^2 \ln m_{\sigma}^2} & \text{(broken phase),} \end{cases} \quad (48)$$

where  $\alpha$  is a  $\tilde{\lambda}$ -dependent constant,  $\alpha = \frac{\frac{3}{2}N+3}{(4\pi N\Lambda)^2 \ln 4} \tilde{\lambda}$ . Note that  $m_{\sigma}^2 = -2\mu^2$  for  $\mu^2 < 0$ . One immediately finds that the “critical exponents” are not constants as the conventional quantum critical phenomena suggests; instead they are related to the mass squared scale itself, and tends to 0 at  $\mu^2 \rightarrow 0$ .

Moreover, one can find in Fig. 4 that the entanglement entropy reduces as  $\mu^2$  is tuned up. This is because when the system departs from quantum critical point as  $\mu^2$  increases from 0, the correlation length  $\xi \sim \mu^{-1}$  decreases, and hence the level of entanglement reduces. The entanglement entropy has a finite local maximum with a cusp at the phase transition point  $\mu^2 = 0$ . This result is in agreement qualitatively with [3] for the Ising Model.

Such behavior of the entanglement entropy can also be interpreted from the point of view of lattice models. The spatial derivative term in action of field theory is regarded as the key

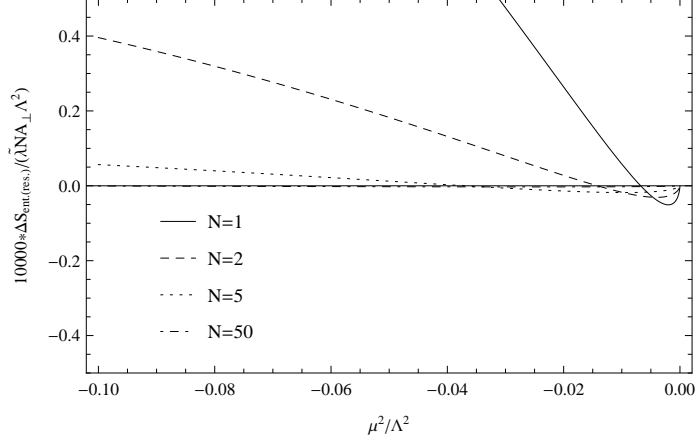


Figure 5.  $\lambda$ -dependent subleading part of the entanglement entropy at  $O(\lambda)$  in the symmetry broken phase. Note that this plot is  $\tilde{\lambda}$ -independent, as it is in units of  $N\tilde{\lambda}A_{\perp}\Lambda^2$ , magnified by a factor of 10000.

for producing non-trivial entanglement. In the lattice models, the spatial derivative term corresponds to the difference between the fields at one site and its nearest neighbor, which is called the lattice link. Without the lattice links, the vacuum of the total system would be just the direct product of local oscillator's vacuum at each site,

$$|\Omega\rangle = |0\rangle_1 \otimes |0\rangle_2 \otimes \dots, \quad (49)$$

i.e. there is no entanglement. However, when the lattice link is present, vacuum can be the non-trivial superposition of the oscillator's state at each site.

$$|\Omega\rangle = \sum_{i_1 i_2 \dots} c_{i_1 i_2 \dots} |\phi_{i_1}(1)\rangle \otimes |\phi_{i_2}(2)\rangle \otimes \dots, \quad (50)$$

where  $|\phi_{i_1}(1)\rangle$  is the  $i$ -th state of oscillator at site  $i$ .

On the other hand, the mass term in the action corresponds to the harmonic potential for the oscillators at each site. As the mass increases, the potential wall becomes more steep, which enhances on-site localization and suppresses hopping. The tunneling of quantum fluctuations is also suppressed. All these effects reduce the level of entanglement against increasing  $\mu^2$ .

When the number of  $\phi$  species  $N > 1$ , the Goldstone bosons emerge in the symmetry broken phase. The contribution to the entanglement entropy from each Goldstone mode is fixed and independent of  $\mu^2$ , as been demonstrated in (38). On the contrary, the massive

mode always has  $N = 1$  contribution. Therefore as the mass-varying contribution from  $\sigma$  is suppressed by increasing  $N$ , and becomes flatter. While  $N \rightarrow \infty$ , entanglement entropy in the broken phase is dominated by the massless Goldstone bosons, and becomes completely flat in the plot.

## VI. DISCUSSION, CONCLUSION AND OUTLOOK

In this paper, we perturbatively calculate the entanglement entropy of  $O(N)$   $\sigma$ -model with spontaneous symmetry breaking of  $O(N)$  by tuning  $\mu^2$  from being positive to negative in 3+1 dimensions, up to the  $O(\lambda)$  order. The entanglement entropy of this model in the symmetric phase is given in (28), while in the broken phase it becomes (47). These two expressions are combined in (1). We find that the area law is preserved in the quantum phase transition. However, due to the emergence of the cubic interactions, the subleading structure changes from log in  $O(N)$  symmetric phase to log squared in the broken phase. We also numerically display the behavior of the entanglement entropy against  $\mu^2$ , as shown in Fig. 4. There occurs a cusped peak at the quantum phase transition point  $\mu^2 = 0$ . While  $|\mu^2|$  shifts away from 0, the level of entanglement reduces, in both phases. This implies that such behavior of the entanglement entropy can be regarded as the signature signifying the quantum phase transition in the  $O(N)$   $\sigma$ -model with the order parameter  $\langle\sigma\rangle$ .

Generally speaking, in the quantum field theory calculation, each quantum loop gives rise to a log divergence. The calculation for the symmetric phase (Section III) shows that the two-loops of  $\phi$ 's in general yield the  $(\log)^2$  divergence, but one of the double logs is canceled by the counter terms under the on-shell mass renormalization conditions, leaving the single log result in (28). In the broken phase (Section IV), similar cancellation happens for the two-loop diagrams with one vertex due to the quartic interaction (in the left column of Fig. 2) under the corresponding on-shell renormalization conditions<sup>2</sup>. However, the double log divergences of the two-loops with two vertices at  $x$  and  $x'$  due to the cubic interactions (in the middle column of Fig. 2) can not be canceled by the counter terms, yielding the log squared structure in the entanglement entropy expression in (47). The double log structure does not appear in [22] because their approximation assumes that the  $x \rightarrow x'$  part dominates the Green's function on the cone, which simplifies the sunset

---

<sup>2</sup> see the Appendix for the details.

diagrams from the cubic interactions in the middle column of Fig. 2 to the one-vertex two-loop diagrams in the left column of the same figure. We had argued that this approximation is incorrect in the last paragraph of Section IV. If we take into account the " $x$  away from  $x'$ " contribution, the log squared divergence appears naturally. Note that the log and the double log structures do not depend on the renormalization schemes because they are of order  $\tilde{\lambda}$  quantities. The effect of different schemes will take place at  $O(\tilde{\lambda}^2)$  above.

In the expression of the entanglement entropy of our paper, we employ the renormalized mass and coupling constant in the tree level, such that the final result is expressed in terms of these renormalized parameters. From this point of view, our results of the log divergence and the coefficients in  $S_{\text{ent.}}$  of the  $O(N)$  symmetric phase is consistent with those in [22] in terms of bare parameters. Despite that our renormalization prescription is different from [22]'s, but they should be equivalent. This is because their cutoff dependence in the  $\lambda$ -independent subleading part is hidden in the renormalized mass, i.e.  $m_r^2 = m_{\text{bare}}^2 + \delta m^2(\Lambda)$ , while we use renormalized parameters since the tree level, so that in our corresponding part the cutoff dependence is manifest. These two results in fact describe the same physics.

The behavior of the entanglement entropy under spontaneous symmetry breaking had been studied in some quantum systems, for example [32, 33]. [32] shows that, for the bi-partite 1+1 dimensional Heisenberg ferromagnet with spontaneously broken global symmetry, the entanglement entropy in general diverges as  $\frac{n}{2} \log m$  as  $m$  is large, where  $m$  is the number of the local degrees of freedom and is related to the subsystem size  $l$  by  $m = l^d$ , and  $n$  is interpreted as the number of zero-energy Goldstone bosons. In 1+1 dimensions, the boundary between the bipartite subsystems is a point; as a result, the area law is replaced by a log. In our model, the subsystem size  $l$  is infinitely large, and therefore we don't have the finite volume ( $l^d$ ) contribution in the entanglement entropy. [33] deals with the  $O(N)$  quantum non-linear sigma models in a finite volume of size  $L$  in  $d + 1 \geq 2 + 1$  dimensions. The  $O(N)$  symmetry is spontaneously broken into  $O(N - 1)$  and the Goldstone bosons pick up an induced mass by applying a small external field  $\vec{h}$ . The entanglement entropy between the bipartite subsystems is calculated by the wave function method. For the cases of a smooth boundary in  $d = 2$  and a straight boundary in  $d = 3$  between the subsystems, the entanglement entropy they obtain has a power law lead term divergent with the cutoff scale  $a$  exhibiting the area law,  $A_{\perp}/a^{d-1}$ , and a subleading log term divergent with  $L$ ,  $\log(\rho_s L/c)$ , where  $\rho_s$  comes from the Goldstone boson mass due to explicit symmetry breaking and  $c$  is



the Goldstone boson velocity. The coefficient of the log term is proportional to the number of the Goldstone modes. Their model is the so-called non-linear sigma model as their  $\sigma$  field is taken to be infinitely heavy and hence integrated out. In our model, the Goldstone bosons remain massless so we do not see this subleading log term, while the massive  $\sigma$  field in our model is included, giving rise to our double log term (due to the cubic interaction) and log term (due to the quartic interaction) in the broken phase. The absence of the massive  $\sigma$  field in [33] also explains why their entanglement entropy lacks our double log term.

There are many interesting directions to be explored based on this work. Straight forward generalization includes introducing the gauge fields into the  $O(N)$   $\sigma$ -model, imposing a chemical potential, or external electric-magnetic fields, and then study the quantum phase transition in terms of entanglement. Such a system would be more complicated yet more realistic. Moreover, in high energy physics, pion gas with isospin chemical potential has quantum phase transition into Bose-Einstein condensate, which is also of interest to study from the perspective of entanglement entropy.

## ACKNOWLEDGMENTS

The authors would like to thank Feng-Li Lin, Qun Wang and Shi Pu for helpful discussions. This work is supported by the MOST, NTU-CTS and the NTU-CASTS of Taiwan. JWC is partly supported by the Ministry of Science and Technology, Taiwan, under Grant No. 108-2112-M-002-003-MY3 and the Kenda Foundation.

## APPENDIX: RENORMALIZATION OF $O(N)$ MODEL AND ENTANGLEMENT ENTROPY

In the symmetric phase, the action of  $O(N)$  sigma-model is composed of the renormalized part and the counter terms,

$$\begin{aligned} \mathcal{L} = & \sum_{i=1}^N \left[ \frac{1}{2} (\partial\phi^i)^2 - \frac{1}{2} \mu^2 (\phi^i)^2 \right] - \frac{\lambda}{4} \left[ \sum_{i=1}^N (\phi^i)^2 \right]^2 \\ & + \sum_{i=1}^N \left[ \frac{1}{2} \delta Z (\partial\phi^i)^2 - \frac{1}{2} \delta \mu^2 (\phi^i)^2 \right] - \frac{\delta \lambda}{4} \left[ \sum_{i=1}^N (\phi^i)^2 \right]^2, \end{aligned} \quad (51)$$

where

$$\begin{aligned}
\delta Z &= O(\lambda^2), \\
\delta\mu^2 &= \lambda \delta^{(1)}\mu^2 + O(\lambda^2), \\
\delta\lambda &= \lambda^2 \delta^{(2)}\lambda + O(\lambda^3)
\end{aligned} \tag{52}$$

denote the wave-function, mass, and coupling constant counter terms expanded w.r.t.  $\lambda$ . The superscripts (1), (2) in  $\delta^{(1)}\mu^2$  and  $\delta^{(2)}\lambda$  label the coefficients of the corresponding  $\lambda$  expansion order of  $\delta\mu^2$  and  $\delta\lambda$  respectively. It can be demonstrated that wave-function renormalization counter term  $\delta Z$  and the coupling renormalization counter term are no less than second order. In  $O(\lambda)$ , only the mass renormalization counter term  $\delta\mu^2$  is involved. So we have,

$$\begin{aligned}
\mathcal{L} &= \sum_{i=1}^N \left[ \frac{1}{2} (\partial\phi^i)^2 - \frac{1}{2} \mu^2 (\phi^i)^2 \right] - \frac{\lambda}{4} \left[ \sum_{i=1}^N (\phi^i)^2 \right]^2 \\
&\quad - \sum_{i=1}^N \left[ \frac{1}{2} \delta\mu^2 (\phi^i)^2 \right]
\end{aligned} \tag{53}$$

up to  $O(\lambda)$ . After the SSB, however, the fields split into

$$(\phi^1, \phi^2, \dots, \phi^{N-1}, \phi^N) = (0, 0, \dots, 0, \frac{m_\sigma}{\sqrt{2\lambda}}) + (\pi^1, \pi^2, \dots, \pi^{N-1}, \sigma). \tag{54}$$

where  $m_\sigma = \sqrt{-2\mu^2}$ , and the Lagrangian with the counter terms in (51) becomes

$$\begin{aligned}
\mathcal{L} &= \sum_{i=1}^{N-1} \left[ \frac{1}{2} (\partial\pi^i)^2 \right] + \left[ \frac{1}{2} (\partial\sigma)^2 - \frac{1}{2} m_\sigma^2 \sigma^2 \right] \\
&\quad - \frac{\lambda}{4} \left[ \sum_{i=1}^{N-1} (\pi^i)^2 \right]^2 - \frac{\lambda}{4} \sigma^4 - \frac{\lambda}{2} \left[ \sum_{i=1}^{N-1} (\pi^i)^2 \right] \sigma^2 \\
&\quad - \sqrt{\frac{\lambda}{2}} m_\sigma \left[ \sum_{i=1}^{N-1} (\pi^i)^2 \right] \sigma - \sqrt{\frac{\lambda}{2}} m_\sigma \sigma^3 \\
&\quad - \frac{\lambda}{2} \left[ \delta^{(1)}\mu^2 + \frac{1}{2} m_\sigma^2 \delta^{(2)}\lambda \right] \sum_{i=1}^{N-1} [(\pi^i)^2] \\
&\quad - \frac{\lambda}{2} \left[ \delta^{(1)}\mu^2 + \frac{3}{2} m_\sigma^2 \delta^{(2)}\lambda \right] \sigma^2 \\
&\quad - \sqrt{\frac{\lambda}{2}} m_\sigma \left[ \delta^{(1)}\mu^2 + \frac{1}{2} m_\sigma^2 \delta^{(2)}\lambda \right] \sigma + O(\lambda^2).
\end{aligned} \tag{55}$$

up to  $O(\lambda)$ . By demanding the 1-loop mass correction be zero (see (57) below) and the tadpole contribution (67) vanish, the two different combinations of the coefficients in the

counter terms in the last three lines of (55) are fixed, and the infinity in this Lagrangian is canceled. The calculation is in the following.

The renormalization scheme depends on the renormalization condition. To fix the mass renormalization counter terms which appear in both the symmetric and the broken phases, we choose the on-shell mass renormalization condition, such that the renormalized masses of  $\phi$  (in the symmetric phase) and  $\sigma$  (in the broken phase) equal to their tree level ones respectively. Assuming the propagator takes the form  $G^{-1}(p^2) = p^2 + M^2(p^2)$ .

As a result, in the symmetric phase,  $\phi$  physical mass is defined by the renormalization condition

$$M_\phi^2(p^2 = \mu^2) = \mu^2, \quad (56)$$

and in the broken phase,  $\sigma$  physical mass is fixed by

$$M_\sigma^2(p^2 = m_\sigma^2) = m_\sigma^2 = -2\mu^2. \quad (57)$$

In the  $O(N)$  symmetric phase, the entanglement entropy of the scalar field theory in  $3+1$  dimensions is UV divergent,

$$S_{\text{ent.}}(\mu^2, \lambda) = \#A_\perp \Lambda^2 [(a_0 + a_1 \lambda) + (b_0 + b_1 \lambda) \left( \frac{|\mu^2|}{\Lambda^2} \right) \ln \left( \frac{|\mu^2|}{\Lambda^2} \right) + O \left( \lambda^2, \frac{|\mu^2|}{\Lambda^2} \right)], \quad (58)$$

where  $\Lambda$  is cut-off of momentum. This is indeed the case for the  $O(N)$   $\sigma$ -model in symmetric phase. As  $|\mu^2|/\Lambda^2 \rightarrow 0$ , the leading order is  $a_0 + a_1 \lambda + O(\lambda^2)$ , while the subleading order is

$$(b_0 + b_1 \lambda + O(\lambda^2)) \left( \frac{|\mu^2|}{\Lambda^2} \right) \ln \left( \frac{|\mu^2|}{\Lambda^2} \right).$$

In this phase, the wave-function and the coupling renormalization counter terms are not involved, so the renormalization condition at  $O(\lambda)$  level is given by

$$M_{\phi,(0)}^2 + M_{\phi,(1)}^2 \lambda + O(\lambda^2) = \mu^2, \quad (59)$$

where

$$M_{\phi,(0)}^2 = \mu^2, \quad (60)$$

$$M_{\phi,(1)}^2 = N [\delta^{(1)} \mu^2 + (N+2)G_\phi(0)]. \quad (61)$$

Thus, we have

$$\delta \mu^2 = -\lambda(N+2)G_\phi(0) + O(\lambda^2). \quad (62)$$

The  $S_{\text{ent.}}$  can be expressed by the transverse mass  $m_{\perp}^2$ ,

$$S_{\text{ent.}}(\mu^2 > 0) = -\frac{NA_{\perp}}{12} \int \frac{d^2p_{\perp}}{(2\pi)^2} \ln \frac{p_{\perp}^2 + m_{\perp}^2(\mu^2)}{p_{\perp}^2 + \Lambda^2}. \quad (63)$$

With the counter term, the transverse mass is just renormalized mass,

$$\begin{aligned} m_{\perp}^2 &= \mu^2 + \lambda(N+2)G_{\phi}(0) + \lambda\delta^{(1)}\mu^2 + O(\lambda^2) \\ &= \mu^2 + O(\lambda^2). \end{aligned} \quad (64)$$

If we express the entanglement entropy in the following general form,

$$S_{\text{ent.}}(\mu^2 > 0) = \#A_{\perp}\Lambda^2 \left[ (a_0 + a_1\lambda) + (b_0 + b_1\lambda) \left( \frac{\mu^2}{\Lambda^2} \right) \ln \left( \frac{\mu^2}{\Lambda^2} \right) + O \left( \lambda^2, \frac{\mu^2}{\Lambda^2} \right) \right], \quad (65)$$

the coefficients then are

$$\begin{aligned} a_0 &= N \log 4, \\ b_0 &= N, \\ a_1 = b_1 &= 0. \end{aligned} \quad (66)$$

In the broken phase, to fix the coupling constant renormalization counter terms which now appear at the leading order, we use the on-shell mass renormalization condition (57) along with the requirement that the tadpole contribution of  $\sigma$  vanishes,

$$\langle \sigma(x) \rangle = V_{\sigma} G_{\sigma}(x) = 0, \quad (67)$$

where the tadpole VEV is decomposed into the coefficient  $V_{\sigma}$  and the Green's function  $G_{\sigma}(x)$ . They give rise to the conditions

$$M_{\sigma,(0)}^2 + M_{\sigma,(1)}^2(p^2 = m_{\sigma}^2)\lambda + O(\lambda^2) = m_{\sigma}^2, \quad (68)$$

$$V_{\sigma,(0)} + V_{\sigma,(1)}\sqrt{\lambda} + O(\lambda) = 0, \quad (69)$$

where the subscripts (1), (2) denotes the coefficients of the corresponding order in  $\lambda$  expansion.

sions. We find

$$M_{\sigma,(0)}^2 = m_\sigma^2, \quad (70)$$

$$\begin{aligned} M_{\sigma,(1)}^2(p^2 = m_\sigma^2) &= 3G_\sigma(0) + (N-1)G_\pi(0) \\ &\quad - 9m_\sigma^2 L_\sigma(p^2 = m_\sigma^2) - (N-1)m_\sigma^2 L_\pi(p^2 = m_\sigma^2) \\ &\quad + \left( \delta^{(1)}\mu^2 + \frac{3}{2}m_\sigma^2 \delta^{(2)}\lambda \right), \end{aligned} \quad (71)$$

$$V_{\sigma,(0)} = 0, \quad (72)$$

$$\begin{aligned} V_{\sigma,(1)} &= -\frac{m_\sigma}{\sqrt{2}} [3G_\sigma(0) + (N-1)G_\pi(0) \\ &\quad + \left( \delta^{(1)}\mu^2 + \frac{1}{2}m_\sigma^2 \delta^{(2)}\lambda \right)] , \end{aligned} \quad (73)$$

in which  $L(p^2)$  is defined by

$$L(p^2) = \int \frac{d^4 q}{(2\pi)^4} G(p-q) G(q). \quad (74)$$

Thus, we have

$$\begin{aligned} \delta\mu^2 &= -\lambda [3G_\sigma(0) + (N-1)G_\pi(0) \\ &\quad + \frac{9}{2}m_\sigma^2 L_\sigma(p^2 = m_\sigma^2) + \frac{1}{2}(N-1)m_\sigma^2 L_\pi(p^2 = m_\sigma^2)] + O(\lambda^2), \end{aligned} \quad (75)$$

$$\delta\lambda = \lambda^2 [9L_\sigma(p^2 = m_\sigma^2) + (N-1)L_\pi(p^2 = m_\sigma^2)] + O(\lambda^3). \quad (76)$$

Now the entanglement entropy reads

$$\begin{aligned} S_{\text{ent.}}(\mu^2 < 0) &= -\frac{A_\perp}{12} \int \frac{d^2 p_\perp}{(2\pi)^2} \ln \frac{p_\perp^2 + m_{\sigma,\perp}^2(m_\sigma^2)}{p_\perp^2 + \Lambda^2} \\ &\quad - \frac{(N-1)A_\perp}{12} \int \frac{d^2 p_\perp}{(2\pi)^2} \ln \frac{p_\perp^2 + m_{\pi,\perp}^2(m_\sigma^2)}{p_\perp^2 + \Lambda^2} \\ &\quad + \lambda \frac{A_\perp}{12} \int \frac{d^2 p_\perp}{(2\pi)^2} \frac{m_\sigma^2}{p_\perp^2 + m_\sigma^2} [D_\sigma(p_\perp^2, q^2) + (N-1)D_\pi(p_\perp^2, q^2)] \Big|_{q^2=m_\sigma^2} \\ &\quad + \lambda \frac{(N-1)A_\perp}{12} \int \frac{d^2 p_\perp}{(2\pi)^2} \frac{m_\sigma^2}{p_\perp^2 + m_\sigma^2} [D_{\pi\sigma}(p_\perp^2, q^2)] \Big|_{q^2=0} + O(\lambda^2), \end{aligned} \quad (77)$$

where

$$\begin{aligned}
D_\sigma(p_\perp^2, q^2) &= 9 \int \frac{d^2 k_\parallel}{(2\pi)^2} \frac{d^2 k_\perp}{(2\pi)^2} \frac{1}{k^2 + m_\sigma^2} \left[ \frac{1}{k_\parallel^2 + (\mathbf{k}_\perp + \mathbf{p}_\perp)^2 + m_\sigma^2} - \frac{1}{(\mathbf{k} + \mathbf{q})^2 + m_\sigma^2} \right] \\
&= 9 [\Gamma_\sigma(p_\perp^2) - L_\sigma(q^2)], \tag{78}
\end{aligned}$$

$$\begin{aligned}
D_\pi(p_\perp^2, q^2) &= \int \frac{d^2 k_\parallel}{(2\pi)^2} \frac{d^2 k_\perp}{(2\pi)^2} \frac{1}{k^2} \left[ \frac{1}{k_\parallel^2 + (\mathbf{k}_\perp + \mathbf{p}_\perp)^2} - \frac{1}{(\mathbf{k} + \mathbf{q})^2} \right] \\
&= \Gamma_\pi(p_\perp^2) - L_\pi(q^2), \tag{79}
\end{aligned}$$

$$\begin{aligned}
D_{\pi\sigma}(p_\perp^2, q^2) &= 2 \int \frac{d^2 k_\parallel}{(2\pi)^2} \frac{d^2 k_\perp}{(2\pi)^2} \frac{1}{k^2 + m_\sigma^2} \left[ \frac{1}{k_\parallel^2 + (\mathbf{k}_\perp + \mathbf{p}_\perp)^2} - \frac{1}{(\mathbf{k} + \mathbf{q})^2} \right] \\
&= 2 [\Gamma_{\pi\sigma}(p_\perp^2) - L_{\pi\sigma}(q^2)]. \tag{80}
\end{aligned}$$

The explicit calculation of  $D$  is shows that

$$\begin{aligned}
D_\sigma(p_\perp^2, q^2) &= \int \frac{d^2 k_\parallel}{(2\pi)^2} \frac{d^2 k_\perp}{(2\pi)^2} \frac{9}{k^2 + m_\sigma^2} \left[ \frac{1}{k^2 + m_\sigma^2 + 2\mathbf{k}_\perp \cdot \mathbf{p}_\perp + p_\perp^2} - \frac{1}{k^2 + m_\sigma^2 + 2\mathbf{k} \cdot \mathbf{q} + q^2} \right] \\
&= 9 \int \frac{d^4 l}{(2\pi)^4} \int_0^1 dx \left[ \left( \frac{1}{l^2 + m_\sigma^2 - x^2 p_\perp^2 + x p_\perp^2} \right)^2 - \left( \frac{1}{l^2 + m_\sigma^2 - x^2 q^2 + x q^2} \right)^2 \right] \\
&= \frac{9}{(4\pi)^2} \int_0^1 dx \ln \left( \frac{m_\sigma^2 + x(1-x)q^2}{m_\sigma^2 + x(1-x)p_\perp^2} \right), \tag{81}
\end{aligned}$$

$$\begin{aligned}
D_\pi(p_\perp^2, q^2) &= \int \frac{d^2 k_\parallel}{(2\pi)^2} \frac{d^2 k_\perp}{(2\pi)^2} \frac{1}{k^2} \left[ \frac{1}{k^2 + 2\mathbf{k}_\perp \cdot \mathbf{p}_\perp + p_\perp^2} - \frac{1}{k^2 + 2\mathbf{k} \cdot \mathbf{q} + q^2} \right] \\
&= \int \frac{d^4 l}{(2\pi)^4} \int_0^1 dx \left[ \left( \frac{1}{l^2 - x^2 p_\perp^2 + x p_\perp^2} \right)^2 - \left( \frac{1}{l^2 - x^2 q^2 + x q^2} \right)^2 \right] \\
&= \frac{1}{(4\pi)^2} \ln \left( \frac{q^2}{p_\perp^2} \right), \tag{82}
\end{aligned}$$

$$\begin{aligned}
D_{\pi\sigma}(p_\perp^2, q^2) &= 2 \int \frac{d^2 k_\parallel}{(2\pi)^2} \frac{d^2 k_\perp}{(2\pi)^2} \frac{1}{k^2 + m_\sigma^2} \left[ \frac{1}{k^2 + 2\mathbf{k}_\perp \cdot \mathbf{p}_\perp + p_\perp^2} - \frac{1}{k^2 + 2\mathbf{k} \cdot \mathbf{q} + q^2} \right] \\
&= 2 \int \frac{d^4 l}{(2\pi)^4} \int_0^1 dx \left[ \left( \frac{1}{l^2 + (1-x)m_\sigma^2 - x^2 p_\perp^2 + x p_\perp^2} \right)^2 \right. \\
&\quad \left. - \left( \frac{1}{l^2 + (1-x)m_\sigma^2 - x^2 q^2 + x q^2} \right)^2 \right] \\
&= \frac{2}{(4\pi)^2} \int_0^1 dx \ln \left[ \frac{m_\sigma^2 + x q^2}{m_\sigma^2 + x p_\perp^2} \right]. \tag{83}
\end{aligned}$$

The transverse masses of  $\pi$  and  $\sigma$  are

$$m_{\sigma,\perp}^2 = m_\sigma^2 + \lambda \left[ 3G_\sigma(0) + (N-1)G_\pi(0) - 9m_\sigma^2 L_\sigma(p^2 = m_\sigma^2) - (N-1)m_\sigma^2 L_\pi(p^2 = m_\sigma^2) \right] \\ + \lambda \left[ \delta^{(1)}\mu^2 + \frac{3}{2}m_\sigma^2 \delta^{(2)}\lambda \right] + O(\lambda^2), \quad (84)$$

$$m_{\pi,\perp}^2 = \lambda \left[ G_\sigma(0) + (N+1)G_\pi(0) - 2m_\sigma^2 L_{\pi\sigma}(p^2 = 0) \right] \\ + \lambda \left[ \delta^{(1)}\mu^2 + \frac{1}{2}m_\sigma^2 \delta^{(2)}\lambda \right] + O(\lambda^2). \quad (85)$$

The mass of  $\pi$  is always zero. This gives rise to the condition

$$\delta^{(1)}\mu^2 + \frac{1}{2}m_\sigma^2 \delta^{(2)}\lambda = -3G_\sigma(0) - (N-1)G_\pi(0). \quad (86)$$

One can demonstrate that

$$M_\pi^2(p^2 = 0) = 0 + O(\lambda^2), \quad (87)$$

$$m_{\pi,\perp}^2 = 0 + O(\lambda^2). \quad (88)$$

And, by normalizing  $m_\sigma$  at  $q^2 = m_\sigma^2$ , we have

$$m_{\sigma,\perp}^2 = m_\sigma^2 + O(\lambda^2). \quad (89)$$

The explicit calculation of residual part of the entanglement entropy that cannot be

absorbed by mass renormalization shows that  $\Delta S_{\text{ent.}}^{\text{res.}}$  is given by

$$\begin{aligned}
\Delta S_{\text{ent.}}^{\text{res.}} &= +\lambda \frac{A_{\perp}}{12} \int \frac{d^2 p_{\perp}}{(2\pi)^2} \frac{m_{\sigma}^2}{p_{\perp}^2 + m_{\sigma}^2} [D_{\sigma}(p_{\perp}^2, q^2) + (N-1)D_{\pi}(p_{\perp}^2, q^2)]|_{q^2=m_{\sigma}^2} \\
&\quad + \lambda \frac{(N-1)A_{\perp}}{12} \int \frac{d^2 p_{\perp}}{(2\pi)^2} \frac{m_{\sigma}^2}{p_{\perp}^2} [D_{\pi\sigma}(p_{\perp}^2, q^2)]|_{q^2=0} + O(\lambda^2) \\
&= \lambda \frac{A_{\perp}}{12} \int \frac{d^2 p_{\perp}}{(2\pi)^2} \frac{1}{(4\pi)^2} \left\{ \frac{m_{\sigma}^2}{p_{\perp}^2 + m_{\sigma}^2} \left[ 9 \int_0^1 dx \ln \left( \frac{m_{\sigma}^2 + x(1-x)m_{\sigma}^2}{m_{\sigma}^2 + x(1-x)p_{\perp}^2} \right) + (N-1) \ln \left( \frac{m_{\sigma}^2}{p_{\perp}^2} \right) \right] \right. \\
&\quad \left. + \frac{m_{\sigma}^2}{p_{\perp}^2} \left[ 2(N-1) \int_0^1 dx \ln \left( \frac{m_{\sigma}^2}{m_{\sigma}^2 + xp_{\perp}^2} \right) \right] \right\} + O(\lambda^2) \\
&= \frac{A_{\perp}\Lambda^2}{48\pi} \left\{ \frac{\lambda}{(4\pi)^2} \int_0^1 dt \left\{ \frac{\tilde{m}_{\sigma}^2}{t + \tilde{m}_{\sigma}^2} \left[ 9 \int_0^1 dx \ln \left( \frac{\tilde{m}_{\sigma}^2 + x(1-x)\tilde{m}_{\sigma}^2}{\tilde{m}_{\sigma}^2 + x(1-x)t} \right) + (N-1) \ln \left( \frac{\tilde{m}_{\sigma}^2}{t} \right) \right] \right. \right. \\
&\quad \left. \left. + \frac{\tilde{m}_{\sigma}^2}{t} \left[ 2(N-1) \int_0^1 dx \ln \left( \frac{\tilde{m}_{\sigma}^2}{\tilde{m}_{\sigma}^2 + xt} \right) \right] \right\} + O(\lambda^2) \right\} \\
&= \frac{A_{\perp}\Lambda^2}{48\pi} \left\{ \frac{\lambda}{(4\pi)^2} \int_0^1 dt \left\{ \frac{\tilde{m}_{\sigma}^2}{t + \tilde{m}_{\sigma}^2} \left[ -18 \frac{\text{arcth} \sqrt{\frac{t}{t+4\tilde{m}_{\sigma}^2}}}{\sqrt{\frac{t}{t+4\tilde{m}_{\sigma}^2}}} + 9\sqrt{5} \ln \left( \frac{3+\sqrt{5}}{2} \right) + (N-1) \ln \left( \frac{\tilde{m}_{\sigma}^2}{t} \right) \right] \right. \right. \\
&\quad \left. \left. + \frac{\tilde{m}_{\sigma}^2}{t} 2(N-1) \left[ 1 + \left( 1 + \frac{\tilde{m}_{\sigma}^2}{t} \right) \ln \tilde{m}_{\sigma}^2 / (t + \tilde{m}_{\sigma}^2) \right] \right\} + O(\lambda^2) \right\} \\
&= \frac{A_{\perp}\Lambda^2}{48\pi} \left\{ \frac{\lambda}{(4\pi)^2} \left\{ -18\tilde{m}_{\sigma}^2 \text{Sl}_2(\tilde{m}_{\sigma}^2) + \left[ 9\sqrt{5} \ln \left( \frac{3+\sqrt{5}}{2} \right) \right] \tilde{m}_{\sigma}^2 \ln \left( \frac{\tilde{m}_{\sigma}^2 + 1}{\tilde{m}_{\sigma}^2} \right) \right. \right. \\
&\quad \left. \left. + (N-1)\tilde{m}_{\sigma}^2 \left[ \ln \left( \frac{\tilde{m}_{\sigma}^2 + 1}{\tilde{m}_{\sigma}^2} \right) \ln(\tilde{m}_{\sigma}^2) - \text{Li}_2 \left( -\frac{1}{\tilde{m}_{\sigma}^2} \right) \right] \right. \right. \\
&\quad \left. \left. + 2(N-1)\tilde{m}_{\sigma}^2 \left[ -1 + \left( 1 + \tilde{m}_{\sigma}^2 \right) \ln \left( \frac{\tilde{m}_{\sigma}^2 + 1}{\tilde{m}_{\sigma}^2} \right) + \text{Li}_2 \left( -\frac{1}{\tilde{m}_{\sigma}^2} \right) \right] \right\} + O(\lambda^2) \right\} \\
&= \frac{A_{\perp}\Lambda^2}{48\pi} \left\{ \frac{\lambda}{(4\pi)^2} \left\{ -\frac{9}{2}\tilde{m}_{\sigma}^2 \ln^2(\tilde{m}_{\sigma}^2) + O(\tilde{m}_{\sigma}^2) - \left[ 9\sqrt{5} \ln \left( \frac{3+\sqrt{5}}{2} \right) \right] \tilde{m}_{\sigma}^2 \ln(\tilde{m}_{\sigma}^2) + O(\tilde{m}_{\sigma}^2) \right. \right. \\
&\quad \left. \left. + (N-1)\tilde{m}_{\sigma}^2 \left[ -\ln^2(\tilde{m}_{\sigma}^2) + \frac{1}{2}\ln^2(\tilde{m}_{\sigma}^2) + O(\tilde{m}_{\sigma}^2) \right] \right. \right. \\
&\quad \left. \left. + 2(N-1)\tilde{m}_{\sigma}^2 \left[ -\ln(\tilde{m}_{\sigma}^2) - \frac{1}{2}\ln^2(\tilde{m}_{\sigma}^2) + O(\tilde{m}_{\sigma}^2) \right] \right\} + O(\lambda^2) \right\} \\
&= \frac{A_{\perp}\Lambda^2}{48\pi} \left\{ \frac{\lambda}{(4\pi)^2} \left\{ -\left[ \frac{9}{2} + \frac{3}{2}(N-1) \right] \tilde{m}_{\sigma}^2 \ln^2(\tilde{m}_{\sigma}^2) \right. \right. \\
&\quad \left. \left. - \left[ 9\sqrt{5} \ln \left( \frac{3+\sqrt{5}}{2} \right) + 2(N-1) \right] \tilde{m}_{\sigma}^2 \ln(\tilde{m}_{\sigma}^2) \right\} + O(\lambda^2, \tilde{m}_{\sigma}^2) \right\},
\end{aligned}$$

where  $\text{Li}_2$  is the polylog function  $\text{Li}_{\alpha=2}$ , and we also define the function of integral for the  $\sigma$



loop by

$$\text{Sl}_2(\tilde{m}_\sigma^2) = \int_0^1 dt \frac{1}{t + \tilde{m}_\sigma^2} \left[ \frac{\text{arcth} \sqrt{\frac{t}{t+4\tilde{m}_\sigma^2}}}{\sqrt{\frac{t}{t+4\tilde{m}_\sigma^2}}} \right], \quad (90)$$

such that

$$\lim_{x \rightarrow 0} \frac{\text{Sl}_2(x)}{\ln^2 x} = \frac{1}{4}, \quad (91)$$

$$\lim_{x \rightarrow 0} \frac{-\text{Li}_2(-\frac{1}{x})}{\ln^2 x} = \frac{1}{2}. \quad (92)$$

To summarize,

$$\begin{aligned} \Delta S_{\text{ent.}}^{\text{res.}} &= +\lambda \frac{A_\perp}{12} \int \frac{d^2 p_\perp}{(2\pi)^2} \frac{m_\sigma^2}{p_\perp^2 + m_\sigma^2} [D_\sigma(p_\perp^2, q^2) + (N-1)D_\pi(p_\perp^2, q^2)]|_{q^2=m_\sigma^2} \\ &\quad + \lambda \frac{(N-1)A_\perp}{12} \int \frac{d^2 p_\perp}{(2\pi)^2} \frac{m_\sigma^2}{p_\perp^2} [D_{\pi\sigma}(p_\perp^2, q^2)]|_{q^2=0} + O(\lambda^2) \\ &= \frac{A_\perp \Lambda^2}{48\pi} \left\{ \frac{\lambda}{(4\pi)^2} \int_0^1 dt \left\{ \frac{\tilde{m}_\sigma^2}{t + \tilde{m}_\sigma^2} \left[ 9 \int_0^1 dx \ln \left( \frac{\tilde{m}_\sigma^2 + x(1-x)\tilde{m}_\sigma^2}{\tilde{m}_\sigma^2 + x(1-x)t} \right) + (N-1) \ln \left( \frac{\tilde{m}_\sigma^2}{t} \right) \right] \right. \right. \\ &\quad \left. \left. + \frac{\tilde{m}_\sigma^2}{t} \left[ 2(N-1) \int_0^1 dx \ln \left( \frac{\tilde{m}_\sigma^2}{\tilde{m}_\sigma^2 + xt} \right) \right] \right\} + O(\lambda^2) \right\} \\ &= \frac{A_\perp \Lambda^2}{48\pi} \left[ c'_N \lambda \left( \frac{m_\sigma^2}{\Lambda^2} \right) \ln^2 \left( \frac{m_\sigma^2}{\Lambda^2} \right) + c_N \lambda \left( \frac{m_\sigma^2}{\Lambda^2} \right) \ln \left( \frac{m_\sigma^2}{\Lambda^2} \right) + O\left( \lambda^2, \frac{m_\sigma^2}{\Lambda^2} \right) \right], \quad (93) \end{aligned}$$

where

$$c_N = -\frac{1}{(4\pi)^2} [\beta + 2(N-1)], \quad (94)$$

$$c'_N = -\frac{1}{(4\pi)^2} \left[ \beta' + \frac{3}{2}(N-1) \right], \quad (95)$$

with

$$\beta = 9\sqrt{5} \ln \frac{3+\sqrt{5}}{2}, \quad (96)$$

$$\beta' = 18 \lim_{x \rightarrow 0} \frac{1}{\ln^2 x} \int_0^1 dt \frac{1}{t+x} \frac{\text{arcth} \sqrt{\frac{t}{t+4x}}}{\sqrt{\frac{t}{t+4x}}} = \frac{9}{2}. \quad (97)$$

At last, we can see that there is an extra order that is more divergent than  $m_\sigma^2 \log(m_\sigma^2/\Lambda^2)$  but less divergent than 1 as  $m_\sigma^2/\Lambda^2 \rightarrow 0$ . This order comes from all the two-vertex loops due to the cubic interactions.

---

[1] R. Horodecki, P. Horodecki, M. Horodecki and K. Horodecki, *Quantum entanglement*, *Rev.Mod.Phys.* **81** (2009) 865 [quant-ph/0702225].

- [2] V. Vedral, *The role of relative entropy in quantum information theory*, *Rev.Mod.Phys.* **74** (2002) 197 [[quant-ph/0102094](#)].
- [3] T.J. Osborne and M.A. Nielsen, *Entanglement in a Simple Quantum Phase Transition*, *Phys.Rev.* **A66** (2002) 032110.
- [4] G. Vidal, J. Latorre, E. Rico and A. Kitaev, *Entanglement in Quantum Critical Phenomena*, *Phys.Rev.Lett.* **90** (2003) 227902 [[quant-ph/0211074](#)].
- [5] J. Latorre, E. Rico and G. Vidal, *Ground State Entanglement in Quantum Spin Chains*, *Quant.Inf.Comput.* **4** (2004) 48 [[quant-ph/0304098](#)].
- [6] C.-Y. Huang and F.-L. Lin, *Multipartite entanglement measures and quantum criticality from matrix and tensor product states*, *Phys.Rev.A* **81** (2010) 032304.
- [7] L. Borsten, M.J. Duff and P. L  vay, *The black-hole/qubit correspondence: an up-to-date review*, *Class.Quant.Grav.* **29** (2012) 224008 [[arXiv:1206.3166](#)].
- [8] L. Bombelli, R.K. Koul, J. Lee and R.D. Sorkin, *A Quantum Source of Entropy for Black Holes*, *Phys.Rev.* **D34** (1986) 373.
- [9] J. Bardeen, L. Cooper and J. Schrieffer, *Microscopic Theory of Superconductivity*, *Phys.Rev.* **106** (1957) 162.
- [10] J. Bardeen, L. Cooper and J. Schrieffer, *Theory of Superconductivity*, *Phys.Rev.* **108** (1957) 1175.
- [11] R. Laughlin, *Anomalous Quantum Hall effect: An Incompressible Quantum Fluid with Fractionally Charged Excitations*, *Phys.Rev.Lett.* **50** (1983) 1395.
- [12] S. Sondhi, S. Girvin, J. Carini and D. Shahar, *Continuous Quantum Phase Transitions*, *Rev.Mod.Phys.* **69** (1997) 315.
- [13] J.-W. Chen, M. Huang, Y.-H. Li, E. Nakano and D.-L. Yang, *Phase Transitions and the Perfectness of Fluids*, *Phys.Lett.* **B670** (2008) 18 [[0709.3434](#)].
- [14] J.-W. Chen, C.-T. Hsieh and H.-H. Lin, *Minimum Shear Viscosity over Entropy Density at Phase Transition?: A Counterexample*, *Phys. Lett.* **B701** (2011) 327 [[1010.3119](#)].
- [15] L. Amico, R. Fazio, A. Osterloh and V. Vedral, *Entanglement in many-body systems*, *Rev. Mod. Phys.* **80** (2008) 517 [[quant-ph/0703044](#)].
- [16] M.P. Hertzberg and F. Wilczek, *Some Calculable Contributions to Entanglement Entropy*, *Phys. Rev. Lett.* **106** (2011) 050404.
- [17] P. Calabrese and J.L. Cardy, *Entanglement Entropy and Quantum Field Theory*,

- J.Stat.Mech.* **0406** (2004) P06002 [[hep-th/0405152](#)].
- [18] P. Calabrese and J.L. Cardy, *Entanglement Entropy and Conformal Field Theory*, *J.Phys.* **A42** (2009) 504005 [[0905.4013](#)].
  - [19] J. Cardy and C.P. Herzog, *Universal Thermal Corrections to Single Interval Entanglement Entropy for Conformal Field Theories*, *Phys.Rev.Lett.* **112** (2014) 171603 [[1403.0578](#)].
  - [20] C. Holzhey, F. Larsen and F. Wilczek, *Geometric and Renormalized Entropy in Conformal Field Theory*, *Nucl.Phys.* **B424** (1994) 443 [[hep-th/9403108](#)].
  - [21] M.A. Metlitski, C.A. Fuertes and S. Sachdev, *Entanglement Entropy in the  $O(N)$  Model*, *Phys. Rev. B* **80** (2009) 115122.
  - [22] M.P. Hertzberg, *Entanglement Entropy in Scalar Field Theory*, *J.Phys.* **A46** (2013) 015402 [[1209.4646](#)].
  - [23] M. Srednicki, *Entropy and Area*, *Phys.Rev.Lett.* **71** (1993) 666 [[hep-th/0405152](#)].
  - [24] A. Dobado, F.J. Llanes-Estrada and J.M. Torres-Rincon, *Minimum of eta/s and the phase transition of the Linear Sigma Model in the large-N limit*, *Phys. Rev.* **D80** (2009) 114015 [[0907.5483](#)].
  - [25] A. Dobado and J.M. Torres-Rincon, *Bulk viscosity and the phase transition of the linear sigma model*, *Phys. Rev.* **D86** (2012) 074021 [[1206.1261](#)].
  - [26] X.-G. Wen, *Topological Orders in Rigid States*, *Int.J.Mod.Phys.* **B4** (1990) 239.
  - [27] H.-C. Jiang, Z. Wang and L. Balents, *Identifying Topological Order by Entanglement Entropy*, *Nature Physics* **8** (2012) 902.
  - [28] W. Li, A. Weichselbaum and J.v. Delft, *Identifying Symmetry-protected Topological Order by Entanglement Entropy*, *Phys.Rev.B* **88** (2013) 245121.
  - [29] A. Kitaev and J. Preskill, *Topological entanglement entropy*, *Phys. Rev. Lett.* **96** (2006) 110404 [[hep-th/0510092](#)].
  - [30] M. Levin and X.-G. Wen, *Detecting Topological Order in a Ground State Wave Function*, *Phys. Rev. Lett.* **96** (2006) 110405 [[cond-mat/0510613](#)].
  - [31] J.-W. Chen and J.-Y. Pang, *On the Renormalization of Entanglement Entropy*, [1709.03205](#).
  - [32] O.A. Castro-Alvaredo and B. Doyon, *Entanglement entropy of highly degenerate states and fractal dimensions*, *Phys. Rev. Lett.* **108** (2012) 120401 [[1103.3247](#)].
  - [33] M.A. Metlitski and T. Grover, *Entanglement Entropy of Systems with Spontaneously Broken Continuous Symmetry*, [1112.5166](#).

- [34] J.-W. Chen, J. Deng, H. Dong and Q. Wang, *Shear and bulk viscosities of a gluon plasma in perturbative QCD: Comparison of different treatments for the  $gg \rightarrow ggg$  process*, *Phys. Rev.* **C87** (2013) 024910 [1107.0522].
- [35] J.-W. Chen, Y.-H. Li, Y.-F. Liu and E. Nakano, *QCD viscosity to entropy density ratio in the hadronic phase*, *Phys. Rev.* **D76** (2007) 114011 [hep-ph/0703230].
- [36] J.-W. Chen and E. Nakano, *Shear viscosity to entropy density ratio of QCD below the deconfinement temperature*, *Phys. Lett.* **B647** (2007) 371 [hep-ph/0604138].
- [37] R.A. Lacey, N.N. Ajitanand, J.M. Alexander, P. Chung, W.G. Holzmann, M. Issah et al., *Has the QCD Critical Point been Signaled by Observations at RHIC?*, *Phys. Rev. Lett.* **98** (2007) 092301 [nucl-ex/0609025].
- [38] L.P. Csernai, J. Kapusta and L.D. McLerran, *On the Strongly-Interacting Low-Viscosity Matter Created in Relativistic Nuclear Collisions*, *Phys. Rev. Lett.* **97** (2006) 152303 [nucl-th/0604032].
- [39] J.-W. Chen, S.-H. Dai and J.-Y. Pang, *Strong Coupling Expansion of the Entanglement Entropy of Yang-Mills Gauge Theories*, *Nucl. Phys. B* **951** (2020) 114892 [1503.01766].